

1
2
3
4
5
6
7
8
9
10

11 **mRNA Poly(A)-tail Changes Specified
12 by Deadenylation Broadly Reshape Translation
13 in Drosophila Oocytes and Early Embryos**

14
15
16
17
18
19
20

21 **Stephen W. Eichhorn^{1,2,3}, Alexander O. Subtelny^{1,2,3,4}, Iva Kronja², Jamie C.
22 Kwasnieski^{1,2}, Terry L. Orr-Weaver^{2,3}, and David P. Bartel^{1,2,3}**

23
24
25
26
27
28
29
30

21 ¹Howard Hughes Medical Institute, Whitehead Institute for Biomedical Research, 9
22 Cambridge Center, Cambridge, MA 02142, USA.

23 ²Whitehead Institute for Biomedical Research, 9 Cambridge Center, Cambridge, MA
24 02142, USA.

25 ³Department of Biology, Massachusetts Institute of Technology, Cambridge, MA 02139,
26 USA.

27 ⁴Harvard-MIT Division of Health Sciences and Technology, Cambridge, MA 02139,
28 USA.

31 *Correspondence: dbartel@wi.mit.edu and weaver@wi.mit.edu

32

33 **ABSTRACT**

34 Because maturing oocytes and early embryos lack appreciable transcription,
35 posttranscriptional regulatory processes control their development. To better understand
36 this control, we profiled translational efficiencies and poly(A)-tail lengths throughout
37 Drosophila oocyte maturation and early embryonic development. The correspondence
38 between translational-efficiency changes and tail-length changes indicated that tail-length
39 changes broadly regulate translation until gastrulation, when this coupling disappears.
40 During egg activation, relative changes in poly(A)-tail length, and thus translational
41 efficiency, were largely retained in the absence of cytoplasmic polyadenylation, which
42 indicated that selective poly(A)-tail shortening primarily specifies these changes. Many
43 translational changes depended on PAN GU and Smaug, and both acted primarily
44 through tail-length changes. Our results also revealed the presence of tail-length–
45 independent mechanisms that maintained translation despite tail-length shortening during
46 oocyte maturation, and prevented essentially all translation of *bicoid* and several other
47 mRNAs before egg activation. In addition to these fundamental insights, our results
48 provide valuable resources for future studies.

49

50 **INTRODUCTION**

51 The generation of a zygote through fertilization marks the onset of development for the
52 offspring, and requires the proper completion of sperm and oocyte development in the
53 respective parents. Spermatogenesis produces haploid sperm capable of penetrating the
54 oocyte, whereas oogenesis produces differentiated oocytes that are stockpiled with
55 maternal nutrients, proteins, and mRNAs, and have outer layers that protect the embryo

56 and enable fertilization. In most animals the oocyte is arrested in meiosis, and
57 fertilization leads to initiation of mitosis as the oocyte nucleus completes meiosis and
58 fuses with the haploid sperm nucleus. Fertilization also leads to changes in mRNA
59 translation and protein stability, which support a period of development driven off of
60 maternal stockpiles. After this initial stage of maternal control, which lasts for 1–2
61 mitotic divisions in mammals and 13 mitotic divisions in *Drosophila*, widespread
62 transcription begins from the zygotic nuclei (Tadros and Lipshitz, 2009).

63 The production of viable offspring requires three key developmental events: oocyte
64 maturation, the oocyte-to-embryo transition (OET), and the maternal-to-zygotic transition
65 (MZT) (Figure 1A). Oocyte maturation involves the release of the primary meiotic arrest
66 at prophase I and progression of the oocyte nucleus into meiotic divisions to produce a
67 mature oocyte (egg) capable of being fertilized (Von Stetina and Orr-Weaver, 2011).
68 The mature oocyte is arrested in metaphase II in most vertebrates and metaphase I in
69 insects. The OET requires egg activation, which is coupled to fertilization in most
70 animals. Egg activation releases the secondary meiotic arrest, allowing completion of
71 meiosis (Horner and Wolfner, 2008). The MZT marks the transfer of control of
72 development from the mother to the zygote as maternal mRNAs are degraded,
73 transcription from the zygotic genome begins, and embryonic development becomes
74 dependent on zygotic gene products (Tadros and Lipshitz, 2009). In *Xenopus*, zebrafish,
75 and *Drosophila* the major activation of zygotic transcription occurs as the cell cycle
76 lengthens and gastrulation begins, a developmental period referred to as the midblastula
77 transition.

78 In nearly all animals, oocyte maturation and the OET occur in the absence of
79 transcription, and thus any changes in protein levels must occur through
80 posttranscriptional regulatory mechanisms. Indeed, widespread changes in protein levels
81 without corresponding changes in mRNA levels are observed at these developmental
82 transitions (Kronja et al., 2014a; Kronja et al., 2014b). Posttranscriptional regulation of
83 gene expression during oocyte maturation, the OET, and early embryogenesis faces
84 unique challenges, including stably storing maternal mRNAs through the prolonged
85 periods of oogenesis and maintaining some of these mRNAs in a translationally inactive
86 state (referred to as masking) while selectively translating others at the proper times in
87 development. During mouse oocyte maturation ~1300 mRNAs are translationally
88 upregulated and ~1500 are translationally downregulated (Chen et al., 2011). Similarly,
89 during Drosophila egg activation ~1000 mRNAs are translationally upregulated, and
90 ~500 are translationally repressed (Kronja et al., 2014b).

91 One long-appreciated mechanism of translational regulation during development acts
92 through control of mRNA poly(A)-tail length (Richter, 2007; Weill et al., 2012). The
93 observation of short poly(A) tails in oocytes from amphibians and marine invertebrates
94 led to the proposal that short poly(A) tails help mask maternal mRNAs, preventing
95 translation without triggering the destabilization that typically results from deadenylation.
96 Specific mRNAs are then targeted for cytoplasmic polyadenylation, and the lengthened
97 poly(A) tails in turn cause translational upregulation of these mRNAs (McGrew et al.,
98 1989), as demonstrated for the mRNAs for *mos* and several *cyclin B* genes during oocyte
99 maturation in *Xenopus* (Sheets et al., 1994; Barkoff et al., 1998). The Cytoplasmic
100 Polyadenylation Element Binding Protein (CPEB) plays a critical role in controlling

101 translation of maternal mRNAs, both in recruiting Maskin to repress translation and later
102 in promoting polyadenylation by binding cytoplasmic poly(A) polymerase together with
103 Cleavage and Polyadenylation Specificity Factor (CPSF) (Richter, 2007; Weill et al.,
104 2012; Ivshina et al., 2014). In Drosophila, the cytoplasmic poly(A) polymerase encoded
105 by the *wispy* gene promotes poly(A)-tail lengthening during both oocyte maturation and
106 egg activation (Benoit et al., 2008; Cui et al., 2008; Cui et al., 2013), and increased
107 poly(A)-tail lengths of mRNAs for *cyclin B*, *cortex*, *bicoid*, *torso*, and *Toll* coincide with
108 the translational upregulation of these mRNAs (Salles et al., 1994; Lieberfarb et al.,
109 1996; Vardy and Orr-Weaver, 2007a; Benoit et al., 2008). Moreover, appending
110 synthetic poly(A) tails of increasing lengths to the *bicoid* mRNA promotes the translation
111 of this mRNA, which demonstrates a causal relationship between increased poly(A)-tail
112 length and increased translation in early Drosophila embryos (Salles et al., 1994).

113 Translational repressors, some of which have been identified through genetic analysis
114 of pattern formation in the Drosophila embryo, also act during oogenesis and early
115 embryogenesis (Vardy and Orr-Weaver, 2007b; Besse and Ephrussi, 2008; Barckmann
116 and Simonelig, 2013). These repressors can impact either poly(A)-tail length (Temme et
117 al., 2014), the translational machinery, or both. Brain Tumor and Pumilio (PUM) bind to
118 target mRNAs and recruit the CCR4-NOT deadenylase complex, which shortens poly(A)
119 tails (Kadyrova et al., 2007; Temme et al., 2010; Newton et al., 2015). Bruno binds to
120 target mRNAs during oogenesis and recruits the eIF4E-binding protein Cup, which
121 represses translation by both blocking the interaction between eIF4E and eIF4G
122 (Nakamura et al., 2004) and promoting deadenylation while repressing decapping, which
123 traps mRNAs in a translationally repressed state (Igreja and Izaurralde, 2011). Similarly,

124 the RNA-binding protein Smaug (SMG) is reported to recruit either Cup or the CCR4-
125 NOT deadenylase complex, with the consequent repression of translation (Nelson et al.,
126 2004; Semotok et al., 2005). *smg* mRNA is translationally repressed in the mature oocyte
127 by PUM, and at egg activation this repression is relieved by the PAN GU (PNG) protein
128 kinase complex (Tadros et al., 2007). PNG is also thought to regulate other translational
129 regulators.

130 mRNA expression arrays, RNA-seq and ribosome-footprint profiling have enabled
131 global analyses of mRNA levels and relative translational efficiencies (TEs) in
132 Drosophila oocytes and embryos (Qin et al., 2007; Dunn et al., 2013; Chen et al., 2014;
133 Kronja et al., 2014b). Measuring poly(A)-tail lengths has been more challenging due to
134 the homopolymeric nature of the tail, and this technical hurdle has restricted studies to
135 measuring tail lengths of a small number of Drosophila mRNAs (Salles et al., 1994;
136 Lieberfarb et al., 1996) or to estimating relative differences in tail lengths more broadly
137 using hybridization-based methods (Cui et al., 2013). However, methods are now
138 available to measure poly(A)-tails of essentially any length for millions of individual
139 mRNA molecules (Chang et al., 2014; Subtelny et al., 2014). In zebrafish and Xenopus,
140 high-throughput measurements demonstrate that poly(A)-tail length and TE are globally
141 coupled during early embryonic development (Subtelny et al., 2014), as expected from
142 single-gene studies (McGrew et al., 1989; Sheets et al., 1994; Lieberfarb et al., 1996;
143 Barkoff et al., 1998; Pesin and Orr-Weaver, 2007; Benoit et al., 2008). Surprisingly,
144 however, this coupling disappears at gastrulation and is not observed in any of the post-
145 embryonic samples examined (Subtelny et al., 2014). Thus, soon after a developmental
146 shift in transcriptional control (the MZT), these vertebrate species undergo a

147 developmental shift in translational control, in which TE abruptly changes from being
148 strongly coupled to tail length to being uncoupled.

149 *Drosophila melanogaster* affords the opportunity to define changes in poly(A)-tail
150 length and TE during oocyte maturation, the OET, and the MZT, facilitated by the high
151 quality of both the genome assembly and the coding-sequence (CDS) annotations, the
152 wealth of knowledge on regulatory proteins active during early development, the
153 availability of genetic mutants in these known regulatory proteins, and the ability to
154 isolate sufficient quantities of oocytes and embryos at distinct developmental stages for
155 high-throughput sequencing techniques. Here we systematically analyze changes in
156 poly(A)-tail length and TE during oocyte maturation, the OET and the MZT, and
157 delineate the roles of Wispy, PNG, and SMG in regulating translation during these
158 crucial periods. These studies reveal fundamental insights into the regulatory
159 mechanisms and regimes operating during these key developmental transitions.

160

161 RESULTS

162 A conserved switch in the nature of translational control

163 We performed poly(A)-tail length profiling by sequencing (PAL-seq) (Subtelny et al.,
164 2014) to measure poly(A)-tail lengths globally at eight developmental stages in
165 *Drosophila melanogaster*, beginning with oocytes at the primary meiotic arrest point and
166 ending with embryos late in gastrulation, at germ-band retraction (Figure 1A). PAL-seq
167 determines the poly(A)-tail length of millions of mRNA molecules, providing for each
168 molecule both a fluorescent measurement that reports on the poly(A)-tail length and a
169 sequencing read that reports the cleavage and poly(A) site. Because alternative start sites

170 or alternative splicing can generate different transcripts with the same poly(A) site, we
171 considered our results with respect to a curated set of unique gene models. Moreover,
172 because alternative cleavage and polyadenylation can generate different poly(A) sites for
173 mRNAs from the same gene, we used our PAL-seq data to identify for each gene the
174 alternative isoform with the longest 3' UTR and then combined its tail-length
175 measurements with those of any shorter tandem 3'-UTR isoforms. Thus, the “mRNAs”
176 of our analyses each corresponded to a unique gene model representing a different
177 protein-coding gene and the aggregated tail-length results from many (if not all) of the
178 alternative transcripts from that gene. In parallel, we performed ribosome-footprint
179 profiling and RNA-seq to determine TEs (Ingolia et al., 2009), which also report
180 aggregate results for alternative isoforms, allowing comparison of mean poly(A)-tail
181 length and TE for thousands of mRNAs that passed our quantification cutoffs at each
182 stage.

183 In Drosophila, the first 13 division cycles occur in a nuclear syncytium.
184 Cellularization (at 2–3 hours of embryogenesis) marks completion of the MZT and is
185 immediately followed by the morphogenetic movements of gastrulation. Thus, early
186 embryogenesis is controlled by maternal mRNAs, and based on the studies of mRNAs
187 from a few genes (Salles et al., 1994; Lieberfarb et al., 1996), those with longer poly(A)-
188 tails would be predicted to have higher TEs, as observed in vertebrate systems (Subtelny
189 et al., 2014). Indeed, poly(A)-tail length and TE were correlated in cleavage-stage
190 embryos (0–1 h embryos), and the slope of this relationship was steep, such that small
191 differences in poly(A)-tail length corresponded to large differences in TE (Figure 1B; e.g.,
192 the median TE of mRNAs with a poly(A)-tail length between 70–80 nt was >5 fold

193 greater than that of mRNAs with a poly(A)-tail length between 30–40 nt). Likewise,
194 when progressing through the OET, the changes in TE correlated with the changes in tail
195 length (Figure 1B, 0–1 h embryo / Stage 14 oocyte).

196 Although a positive correlation between poly(A)-tail length and TE persisted in the
197 2–3 h embryos, the slope of this relationship strongly diminished such that the median TE
198 of mRNAs with a poly(A)-tail length between 70–80 nt was <2 fold greater than that of
199 mRNAs with a poly(A)-tail length between 30–40 nt, as expected if poly(A)-tail length
200 changes were no longer used to influence translation in these cellularized and gastrulating
201 embryos. Indeed, the changes in poly(A)-tail length that occurred between cleavage-
202 stage and cellularized embryos were not positively correlated with the changes in TE
203 (Figure 1B, 2–3 h embryo / 0–1 h embryo). The positive correlation between poly(A)-tail
204 length and TE disappeared in subsequent stages of gastrulation (3–4 h embryos and 5–6 h
205 embryos), and although tail lengths changed between these stages, the TE changes
206 spanned a very narrow range (Figure 1B, 3–4 h embryo / 2–3 h embryo and 5–6 h
207 embryo / 3–4 h embryo). The tail-length changes observed between these stages
208 presumably resulted from transcription and mRNA decay as well as deadenylation,
209 whereas those in earlier stages resulted primarily from cytoplasmic polyadenylation and
210 deadenylation.

211 The narrower range of TE values and TE changes following the onset of gastrulation
212 (Figure 1B) was consistent with a diminished role of translational regulation in specifying
213 protein output after the embryo begins to modulate gene expression by altering mRNA
214 abundance. Most importantly, these results showed that the developmental shift in the
215 nature of translational control observed in vertebrates also occurs in flies; in *Drosophila*,

216 just as in zebrafish and *Xenopus* (Subtelny et al., 2014), the coupling between poly(A)-
217 tail length and TE observed in the early embryo disappeared around gastrulation.

218 An analysis of the temporal patterns of translational regulation occurring from the
219 OET through the onset of gastrulation identified several significantly enriched patterns,
220 although all possible patterns were observed (Figure 1—figure supplement 1). Among the
221 five enriched profiles were those for mRNAs that were translationally upregulated at the
222 OET and then stayed elevated during early embryonic development, those for mRNAs
223 that were upregulated at the OET and then downregulated during early embryonic
224 development, and those for mRNAs that were downregulated before the OET and
225 remained repressed (Figure 1—figure supplement 1). Because ribosome-profiling data
226 reflect relative rather than absolute levels of translation of an mRNA across
227 developmental stages, these results should be interpreted as reflecting changes in how
228 well an mRNA was translated relative to all other mRNAs in the same stage. Thus, an
229 mRNA translated at the same absolute efficiency in two stages might be perceived as
230 downregulated if translation of many other mRNAs increased. Nonetheless, these
231 dynamic and substantial changes in TE observed during the OET and early
232 embryogenesis revealed a large-scale and rapid change in the translational capacity of
233 mRNAs relative to each other during early development.

234 Pairwise comparisons within the mRNA, translation, and tail-length datasets (from
235 RNA-seq, ribosome-footprint profiling, and PAL-seq, respectively) for the different
236 developmental stages further supported these overall conclusions (Supplementary File 1).
237 As expected, mRNA abundances were highly correlated between all stages prior to the
238 onset of transcription (Supplementary File 1). Over these same stages, poly(A)-tail

239 lengths for many different mRNAs shortened or lengthened, but these changes seemed to
240 have minimal impact on mRNA abundance measurements, consistent with stability of
241 shorter-tail mRNAs during this time (and also indicating that the poly(A)-selection that
242 was performed as part of the RNA-seq protocol did not bias our RNA abundance, and
243 thus TE, measurements). In contrast to the highly correlated mRNA abundances, the
244 number of ribosome-protected fragments (RPFs) differed substantially between stages
245 prior to the onset of transcription (Supplementary File 1), consistent with dynamic and
246 robust translational regulation during this time. Once transcription began, widespread
247 changes in both mRNA levels and RPFs were observed between stages (Supplementary
248 File 1). Poly(A)-tail lengths varied both prior to and after the onset of transcription, and
249 generally mirrored the pattern of correlations observed for RPFs up until the MZT
250 (Supplementary File 1). Little-to-no positive correlation between poly(A)-tail lengths
251 was observed when comparing samples with no active transcription to those after the
252 onset of robust transcription (Supplementary File 1), presumably because of the influence
253 of nascent transcripts on mean poly(A)-tail lengths.

254 The striking increases in translation observed soon after fertilization presumably
255 generated factors needed for later developmental transitions. For example, translation of
256 mRNAs for *zelda* and *stat92E*, two transcription factors required for the onset of zygotic
257 transcription at the MZT (Liang et al., 2008; Harrison and Eisen, 2015), increased
258 markedly during the OET (Figure 1C), as expected if translational activation of these
259 mRNAs produces the proteins necessary to initiate the MZT, and accounting for the
260 previously noted increase in Zelda protein in early embryos (Harrison and Eisen, 2015).
261 Likewise, translation of *smaug* and *bicoid* mRNA increased markedly during the OET

262 (Figure 1C), yielding factors essential for embryonic development and patterning,
263 respectively. Although translation of *stat92E* and *smaug* began to increase at stage 14,
264 translation of both was still relatively low until after the OET (Figure 1C), consistent with
265 the roles their translation products during early embryonic development.

266

267 **Translational regulation during oocyte maturation**

268 Having established that Drosophila embryos resemble those of fish and frog with respect
269 to the coupling between TE and poly(A)-tail length, we sought to extend these findings to
270 oocytes. The ability to isolate individual oocytes at distinct developmental stages in
271 Drosophila enabled us to measure poly(A)-tail lengths and TEs and examine their
272 relationship at key stages of oogenesis. Stage 11 oocytes are arrested in prophase I.
273 Nuclear envelope breakdown, a hallmark of the release of this arrest, occurs between
274 stages 12 and 13 (Von Stetina et al., 2008; Hughes et al., 2009), and the oocytes arrest in
275 metaphase I during stage 14, the final stage of oogenesis. Thus, comparison of oocytes
276 from stages 11 through 14 captures the events of meiotic progression and oocyte
277 differentiation that occur over the course of oocyte maturation.

278 Poly(A)-tail lengths and TEs were well correlated at stages 11, 12, and 13 ($R_s \geq 0.51$),
279 but poorly correlated at stage 14 ($R_s = 0.20$) (Figure 2). Previously, the relationship
280 between poly(A)-tail length and translation had been examined for the *c-mos* and *cyclin B*
281 mRNAs during Xenopus oocyte maturation (Sheets et al., 1994; Barkoff et al., 1998;
282 Pique et al., 2008). Our results extended these analyses to an invertebrate and to a global
283 scale, showing that, as for the *c-mos* and *cyclin B* mRNAs in the Xenopus oocyte, tail-
284 length increases correspond to translational activation in the maturing Drosophila oocyte.

285 Thus, the global coupling between poly(A)-tail length and TE, which had previously been
286 examined only after fertilization (Subtelny et al., 2014), extends well before fertilization
287 to potentially influence key developmental transitions in the oocyte.

288 Of the mRNAs exceeding our read cutoffs, nearly half (46%) had net TE changes of
289 ≥ 2 fold over the course of oocyte maturation, with mRNAs for 1264 and 1037 genes up-
290 or downregulated, respectively (Figure 2—figure supplement 1A). In contrast, far fewer
291 mRNAs (1.5%) changed in abundance ≥ 2 fold (25 mRNAs increased, and 52 mRNAs
292 decreased), indicating the posttranscriptional nature of this regulation. More detailed
293 comparison of TEs for each mRNA from stages 11 through 14 revealed unexpectedly
294 dynamic and complex temporal patterns of translational control (Figure 3A). The relative
295 TEs for some mRNAs increased progressively at each stage of oogenesis (Figure 3A
296 cluster 1), and this set of mRNAs included *cyclin B* (Figure 3B), whose translational
297 control via polyadenylation is reported to be crucial for oocyte maturation (Benoit et al.,
298 2005). Some of the downregulated mRNAs similarly showed progressive decreases in
299 TE through the stages of oocyte maturation (Figure 3A cluster 26). However, more
300 complex patterns of developmental changes in TE were more commonly observed
301 (Figure 3A). Moreover, changes in TE correlated poorly with previously measured
302 changes in protein abundance (Kronja et al., 2014a), potentially due to a large role of
303 posttranslational regulation during this time (Figure 2—figure supplement 1B, $R_s = 0.15$).

304 The net changes in TE and poly(A)-tail length over the course of oocyte maturation
305 were largely concordant for both translationally up- and downregulated mRNAs,
306 indicating strong coupling between TE and poly(A)-tail length during oocyte maturation
307 (Figure 4A). Nonetheless, a potential deviation from the typical coupled behavior

308 occurred between oocyte stages 13 and 14, when a set of mRNAs that underwent
309 substantial tail-length reductions did not undergo concordant TE reductions (Figure 2,
310 Stage 14 / Stage 13, and Figure 2—figure supplement 2A). These mRNAs tended to
311 have both long poly(A)-tails and efficient translation in stage 13 oocytes, and then
312 remained well translated compared to other mRNAs in stage 14 oocytes, despite
313 undergoing substantial tail shortening (Figure 2—figure supplement 2B). Notable among
314 this set were mRNAs for 22 of the 30 genes encoding subunits of the proteasome (Figure
315 2—figure supplement 2A and B).

316 To examine the relationship between tail-length changes and TE changes for mRNAs
317 of key factors in oocyte maturation, we focused on those of three of the most highly
318 upregulated cell-cycle regulators involved in meiotic progression, Cyclins B and B3 and
319 the Cdc20 ortholog Fizzy (Jacobs et al., 1998; Swan and Schupbach, 2007). Between
320 oocyte stages 11 through 14, the TEs of these mRNAs increased 103, 248, and 319 fold
321 (compared to a median TE change of only 1.3 fold), respectively, whereas poly(A)-tail
322 lengths increased 1.6, 2.4, and 2.0 fold (compared to the median of 1.2 fold) (Figure 4A).
323 In addition to these examples, mRNAs from 121 other genes were very poorly translated
324 in stage 11 oocytes ($TE \leq 0.1$) and became ≥ 10 -fold better translated during oocyte
325 maturation (Figure 2—figure supplement 1C). As with *cyclin B*, *cyclin B3* and *fizzy*
326 mRNAs, these also had modest increases in tail length (Figure 2—figure supplement 1C;
327 median tail-length fold change = 1.7 for mRNAs with $TE \leq 0.1$ in stage 11 oocytes and a
328 ≥ 10 -fold increase in TE in stage 14 oocytes), raising the question of the degree to which
329 modest tail-length increases might explain the large TE increases observed during oocyte
330 maturation.

331 One possibility is that a subset of the mRNAs for a gene underwent extensive
332 polyadenylation, and this change in a subset of mRNAs did not cause much change in the
333 mean tail-length value despite causing a large change in TE. However, for *cyclin B*,
334 *cyclin B3* and *fizzy* mRNAs, the distribution of poly(A)-tail lengths remained unimodal as
335 overall lengths increased, which indicated that the focus on the mean tail-length change
336 in our analyses did not miss specific regulation of a subset of mRNAs for a gene (Figure
337 4B). Also helpful for considering the effects of increasing tail lengths during oocyte
338 maturation is the steep relationship between poly(A)-tail length and TE during this
339 developmental period (Figure 2). The steepness of this relationship in stage 11, 12, and
340 13 oocytes implied a 6- to 7-fold increase in the median TE for mRNAs with a poly(A)-
341 tail length between 70–80 nt relative to those with a poly(A)-tail length between 30–40 nt.
342 In stage 14 oocytes, the poor correlation between tail length and TE resulted in only a
343 1.8-fold increase in median TE when comparing mRNAs with such tail lengths. Thus
344 during oocyte maturation, the modest increases observed in mean poly(A)-tail lengths
345 presumably explain part, but not all, of the robust translational activation of *cyclin B*,
346 *cyclin B3*, *fizzy*, and mRNAs from many other genes. Moreover, a broad range of TE
347 values was observed for mRNAs with the same mean poly(A)-tail length, presumably as
348 a consequence of additional regulatory processes that are independent of poly(A)-tail
349 length. To the extent that these additional processes act concordantly with tail-length-
350 dependent processes, they would increase the apparent effect of tail lengthening.

351

352 **Translational regulation during the oocyte-to-embryo transition**

353 Although egg activation occurs rapidly (within ~20 minutes) (Horner and Wolfner, 2008),
354 this developmental transition induced TE changes for mRNAs from many genes, some of
355 which exceeded 30 fold (Figure 2, lower right) (Kronja et al., 2014b). As in the
356 preceding period of oocyte maturation, tail-length changes corresponded to TE changes
357 (Figure 4A and C). Indeed, during egg activation the correlation between tail-length
358 change and TE change exceeded that observed for any other transition (Figure 1B and
359 Figure 2, lower panels; Figure 4A). Thus during egg activation, changes in poly(A)-tail
360 length can account for a large proportion of the translational changes.

361 mRNAs for the embryonic patterning genes *bicoid*, *torso*, and *Toll* are translationally
362 upregulated during egg activation in a manner reported to depend on changes in poly(A)-
363 tail length (Salles et al., 1994). In our analyses, translation of *bicoid* mRNA was
364 undetectable or detected with very few reads in oocytes from stages 11 through 14, but it
365 became much more highly translated following egg activation, increasing by 36 fold in
366 the activated egg relative to the stage 14 oocyte (median TE change = 1.2 fold). mRNAs
367 for *torso* and *Toll* were somewhat better translated in stage 14 oocytes, but nonetheless
368 their TEs increased 13 and 46 fold, respectively (Figure 4C). During this time, the *Toll*
369 poly(A)-tail length increased 3.3 fold (median tail length change = 1.1 fold), which
370 corresponded well to the trend observed globally for tail-length and TE changes (Figure
371 4C), suggesting that its increased tail-length might fully account for its increased TE.
372 However, concordantly acting tail-length-independent processes that increase the
373 apparent effect of tail-length changes might also be influencing *Toll* translation. Indeed,
374 our subsequent experiments with *wispy*-mutant animals showed that in the absence of
375 cytoplasmic polyadenylation, *Toll* underwent substantial translational upregulation during

376 egg activation and remained one of the most efficiently translated mRNAs in the *wispy*-
377 mutant laid egg, despite having a mean tail length of only 9 nt. The poly(A)-tail lengths
378 of *bicoid* and *torso* increased by only 1.7 and 1.3 fold, respectively, putting them outside
379 the global trend (Figure 4C), and the unimodal tail-length distributions showed again that
380 our focus on the mean change did not miss a unique behavior of a subpopulation of
381 transcripts (Figure 4D). Thus, the translational regulation of these mRNAs seems to also
382 involve tail-length-independent mechanisms.

383 The strong translational upregulation of *bicoid* mRNA, from essentially untranslated
384 in oocytes from stages 11 through 14 to relatively well translated in the activated egg,
385 implied the influence of either a translational repressor acting on *bicoid* mRNA in the
386 oocyte that was relieved at egg activation, or a translational activator acting on it during
387 egg activation. Because *bicoid* mRNA had an average tail length of 42 nt in stage 14
388 oocytes, which was similar to that of many well translated mRNAs at this stage, we
389 conclude that there was likely a translational repressor acting on it in oocytes to prevent
390 its translation prior to egg activation. The same is presumably true for other mRNAs that
391 had little to no detectable translation in oocytes but then became efficiently translated
392 following egg activation. For mRNAs such as *torso*, which had somewhat greater
393 translation in stage 14 oocytes but subsequently experienced a TE increase that was out
394 of proportion to its tail-length increase, either possibility might account for its
395 translational upregulation at egg activation. Likewise, the 15-fold and 4-fold
396 translational activation observed between stage 14 oocytes and 0–1 h embryos for *zelda*
397 and *stat92E*, respectively (Figure 1C), were accompanied by only 1.2-fold changes in
398 poly(A)-tail length for both mRNAs (median TE change = 1.2 fold and median tail length

399 change = 1.1 fold), again implying that a component of their activation may have
400 occurred through a tail-length independent mechanism (note that the poly(A)-tail length
401 of *zelda* was quantified by only 31 and 72 tags in stage 14 oocytes and 0–1 h embryos,
402 respectively).

403

404 **Widespread impact of cytoplasmic polyadenylation on poly(A)-tail lengths but not**
405 **TE**

406 During oocyte maturation and egg activation, changes in poly(A)-tail length occur
407 through the opposing activities of deadenylases and cytoplasmic poly(A)-polymerases,
408 which shorten and lengthen poly(A) tails, respectively (Weill et al., 2012). *Wispy* is the
409 cytoplasmic poly(A)-polymerase responsible for poly(A)-tail lengthening at the end of
410 oocyte maturation and continuing through egg activation (Benoit et al., 2008; Cui et al.,
411 2008). Indeed, within this developmental window, most maternal transcripts bind to
412 oligo(dT) with less affinity in *wispy* mutants, indicating that many poly(A) tails shorten
413 in the absence of *Wispy* (Cui et al., 2013), but the degree to which tail-lengths shorten
414 and the impact on TE had not been previously measured.

415 Our PAL-seq measurements of poly(A)-tail lengths in *wispy*-mutant stage 13 oocytes
416 and laid eggs confirmed the widespread shortening of poly(A) tails in the absence of
417 *Wispy* (Figure 5A). Of the mRNAs from 3571 genes measured in stage 13 oocytes, 1801
418 had tails that were at least 50% shorter in *wispy*-mutant oocytes relative to wild-type, and
419 for all but a few mRNAs the poly(A) tail was at least somewhat shorter in the absence of
420 *Wispy* (Figure 5A). Although *wispy*-mutant eggs do not complete meiosis and thus do
421 not begin nuclear divisions, most of the molecular changes characteristic of the OET are

422 independent of these divisions, motivating a comparison of *wispy*-mutant laid eggs with
423 wild-type early embryos. In *wispy*-mutant laid eggs, 1219 of the 1836 measured mRNAs
424 had poly(A) tails at least 50% shorter than those in the analogous wild-type sample (0–1
425 h embryos), and again for all but a few mRNAs the poly(A) tail was shorter in the
426 absence of Wispy (Figure 5A). Examination of the mRNAs with tails that were least
427 affected by the absence of Wispy revealed a remarkable enrichment for mRNAs of
428 ribosomal proteins, both in oocytes and laid eggs (Figure 5—figure supplement 1A; $p <$
429 10^{-41} and $p < 10^{-44}$, respectively, one-tailed Wilcoxon rank sum test).

430 Strikingly, the global changes in poly(A)-tail length that occurred in the absence of
431 Wispy did not affect the coupling between poly(A)-tail length and TE. In *wispy*-mutant
432 stage 13 oocytes and laid eggs, poly(A)-tail length and TE were correlated to a similar
433 extent as in wild-type oocytes and embryos (Figure 1B, 2, and Figure 5—figure
434 supplement 1B). These correlations were observed even though the RNA-seq
435 measurements used to calculate TEs were made using poly(A)-selected RNA, which in
436 the *wispy*-mutant samples likely resulted in inflated TE estimates for mRNAs with very
437 short poly(A)-tails, as these would be poorly recovered during the poly(A) selection.
438 Indeed, RNA-seq measurements correlated with poly(A)-tail length in the *wispy*-mutant
439 samples but not the wild-type samples (Figure 5—figure supplement 1C), indicating a
440 poly(A)-selection bias in the *wispy*-mutant RNA-seq data but not in the wild-type data.
441 Because neither developmental stage being considered had appreciable transcription or
442 RNA degradation, and because of the poly(A)-selection bias in the *wispy*-mutant RNA-
443 seq data, we reasoned that the RNA-seq measurements from corresponding wild-type
444 samples should most accurately reflect mRNA abundances in the *wispy*-mutant samples.

445 Indeed, results obtained from determining TEs for the *wispy*-mutant samples using the
446 *wispy*-mutant ribosome profiling and the wild-type RNA-seq (Figure 5B) were similar to
447 those obtained when only *wispy*-mutant measurements were used (Figure 5—figure
448 supplement 1B), except they had somewhat stronger correlations between poly(A)-tail
449 length and TE, which supported the idea that these modified TEs more accurately
450 reflected the true TEs at these stages.

451 Importantly, the strong correlation between changes in poly(A)-tail length and
452 changes in TE that occurred at egg activation in wild-type animals was retained in *wispy*-
453 mutant flies (Figures 1B and 5C, respectively), indicating that changes in the length of
454 the poly(A)-tail—not the act of cytoplasmic polyadenylation per se—is what influences
455 TE. Moreover, the changes in TE that occurred during egg activation in *wispy*-mutant
456 samples strongly correlated with those in the wild-type samples, as did the relative
457 changes in poly(A)-tail length (Figure 5D). Thus, although Wispy lengthens the poly(A)-
458 tails of most mRNAs during egg activation, our results indicated that this lengthening
459 was largely dispensable for reshaping TEs during egg activation, as the rank order of tail-
460 length and TE changes at this time were largely preserved in the *wispy*-mutant samples.

461 The observation that cytoplasmic polyadenylation was not needed to generate the
462 rank order of tail-length and TE changes for most mRNAs warranted further investigation,
463 particularly when considering both the critical influence of cytoplasmic polyadenylation
464 for generating these differences during vertebrate development and the importance of
465 Wispy for relieving meiotic arrest during the OET. Perhaps some mRNAs most affected
466 by the loss of Wispy dropped out of our tail-length analysis because they had very short
467 poly(A)-tails in the *wispy* mutant and thus were poorly recovered in our PAL-seq

468 libraries. Although the tail lengths of such mRNAs might have been difficult to measure
469 by PAL-seq, the RPF measurements of mRNAs for all genes can be analyzed without
470 consideration of the corresponding tail-length or mRNA abundance measurements, either
471 of which might selectively lose the set of mRNAs most dependent on Wispy for their
472 regulation. The RPFs in wild-type and *wispy*-mutant stage 13 oocytes were well
473 correlated, and the same was true for 0–1 h wild-type embryos compared with *wispy*-
474 mutant laid eggs ($R_s = 0.76$ for both, Figure 5—figure supplement 1D). Although
475 globally the RPFs were largely preserved in the *wispy*-mutant samples, some mRNAs had
476 many RPFs in the wild-type samples but none in the *wispy*-mutant samples (Figure 5—
477 figure supplement 1D). Included among these was *cortex*, a known target of Wispy, the
478 upregulation of which is essential for the OET (Chu et al., 2001; Benoit et al., 2008).

479 We conclude that during egg activation in Drosophila, cytoplasmic polyadenylation
480 extends the tails of nearly all mRNAs but does not play the major role in generating the
481 relative differences in tail lengths and TEs observed between mRNAs, which implies that
482 poly(A)-tail shortening instead plays the major role in generating these differences.
483 Nonetheless, the mRNAs responsible for the *wispy*-mutant phenotype might be among
484 those that are most strongly dependent on Wispy for their translational state.

485

486 **PNG kinase complex up- and downregulates translation through changes in**
487 **poly(A)-tail length**

488 The PNG kinase, which is required for nuclear divisions in the early embryo, influences
489 the translational up- or downregulation of hundreds of different mRNAs at egg activation
490 (Figure 6A) (Kronja et al., 2014b), presumably through its regulation of translational

491 regulators, such as SMG (Tadros et al., 2007). To characterize the extent to which these
492 downstream regulators might use tail-length changes to influence TE, we profiled
493 poly(A)-tail lengths and TEs in *png*-mutant stage 14 oocytes and activated eggs.
494 Poly(A)-tail lengths and TEs were highly correlated between the *png*-mutant and wild-
495 type stage 14 oocytes, whereas the correlation was substantially lower in *png*-mutant and
496 wild-type activated eggs (Figure 6—figure supplement 1A). Additionally, the poly(A)-
497 tail lengths and TEs in the *png*-mutant activated eggs were quite similar to those in the
498 *png*-mutant stage 14 oocytes, whereas this was not the case for the same comparisons
499 among wild-type samples (Figure 6—figure supplement 1B). The requirement of PNG
500 for achieving the gene-expression profile of the wild-type activated egg but not the stage
501 14 oocyte was consistent with PNG kinase becoming active during egg activation to
502 serve as a master regulator of the OET (Shamanski and Orr-Weaver, 1991; Kronja et al.,
503 2014b).

504 The set of mRNAs dependent on PNG for their translational downregulation was
505 predominantly those that underwent tail-length shortening during egg activation in wild-
506 type samples (median TE \log_2 fold change of -3.03 after median centering and median
507 \log_2 tail-length fold change of -0.35) (Figure 6B). In *png*-mutant embryos, these
508 mRNAs failed to be deadenylated, as expected if tail-length shortening mediated their
509 translational repression (median TE \log_2 fold change of 0.10 after median centering and
510 median \log_2 tail-length fold change of 0.32, which closely resembled the median values
511 for all mRNAs) (Figure 6B). Correspondingly, the set of mRNAs dependent on PNG for
512 their translational upregulation was predominantly those that underwent tail-length
513 extension during wild-type egg activation (median TE \log_2 fold change of 2.98 after

514 median centering and median \log_2 tail-length fold change of 0.62), and these mRNAs
515 failed to undergo tail lengthening in *png* mutants, again as expected if tail-lengthening
516 mediated their translational activation (median TE \log_2 fold change of 0.36 after median
517 centering and median \log_2 tail-length fold change of 0.32, which closely resembled the
518 median values for all mRNAs) (Figure 6C). mRNAs that were translationally up- or
519 downregulated by PNG also typically increased or decreased in poly(A)-tail length,
520 respectively (Figure 6D), and the tail-length changes for either the up- or downregulated
521 sets of mRNAs were largely dependent on PNG (Figure 6B and C), which showed that
522 PNG plays a central role in regulating polyadenylation and deadenylation for the
523 hundreds of mRNAs present at egg activation.

524

525 **SMG-mediated repression occurs primarily through tail shortening and explains**
526 **some but not all of the PNG-mediated translational repression**

527 Because much of the PNG-mediated translational repression is attributed to its
528 derepression of *smg* translation (Tadros et al., 2007), we examined the impact of SMG on
529 the set of mRNAs that depended on PNG for tail-length shortening and translational
530 repression. SMG is reported to downregulate translation of its target mRNAs through
531 either direct recruitment of the deadenylation machinery or recruitment of CUP, which
532 directly represses translation initiation and can also promote deadenylation (Nelson et al.,
533 2004; Semotok et al., 2005; Igreja and Izaurralde, 2011). Our results showed that in the
534 absence of SMG, the poly(A)-tail lengths for the set of PNG-dependent downregulated
535 mRNAs were less shortened during egg activation (median \log_2 tail-length fold changes
536 of -0.22 and -0.04 for the wild-type and *smg* mutant, respectively, relative to the median

537 of all mRNAs, $p < 10^{-27}$, one-tailed Wilcoxon rank sum test), and this coincided with
538 their partial translational derepression (median \log_2 TE fold change of -2.2 and -1.2,
539 respectively, after median centering, $p < 10^{-32}$, one-tailed Wilcoxon rank sum test)
540 (Figure 7A). In contrast, no significant difference was observed for either poly(A)-tail
541 length or TE changes for the PNG-dependent upregulated mRNAs (median \log_2 tail-
542 length fold changes of 0.27 for both the wild-type and *smg* mutant relative to the median
543 of all mRNAs, and median \log_2 TE fold changes of 2.8 and 2.7, respectively, after
544 median centering for the wild-type and *smg* mutant, $p = 0.89$ and 0.37 for tail-length or
545 TE changes, respectively, two-tailed Wilcoxon rank sum test), consistent with SMG
546 functioning only as a repressor (Figure 7B). In general, mRNAs that were translationally
547 repressed by SMG also decreased in poly(A)-tail length, which indicated that recruitment
548 of deadenylases was the dominant mechanism of SMG-dependent translational repression
549 occurring during egg activation and early embryogenesis (Figure 7C). Additionally, in
550 the absence of SMG, a set of mRNAs reported to be bound by SMG in the early embryo
551 (Chen et al., 2014) had longer poly(A) tails and were better translated following the OET
552 (median \log_2 tail-length fold changes of -0.21 and -0.04 for the wild-type and *smg*
553 mutant, respectively, relative to the median of all mRNAs, and median \log_2 TE fold
554 changes of -1.0 and -0.15, respectively, after median centering for the wild-type and *smg*
555 mutant, $p < 10^{-16}$ and 10^{-11} for tail length or TE changes, respectively, one-tailed
556 Wilcoxon rank sum test) (Figure 7—figure supplement 1).

557 Taken together, our results indicate that SMG mediates much of the PNG-dependent
558 translational repression occurring during egg activation and early embryogenesis, with
559 most of this repression occurring through poly(A)-tail shortening. Nevertheless, the

560 residual repression observed in the absence of SMG (Figure 7A) indicates that one or
561 more additional PNG-activated translational repressors also operate at this time.

562

563 **DISCUSSION**

564 Our results from Drosophila oocytes and embryos increase the number of cellular
565 environments known to possess global coupling between poly(A)-tail length and TE,
566 which now include several stages of Drosophila oocytes as well as Drosophila, zebrafish,
567 and Xenopus embryos prior to the onset of gastrulation. At least as early as the primary
568 meiotic arrest point, changes in poly(A)-tail length largely explain changes in TE, and
569 this regulatory strategy continues through early embryonic development. A switch
570 around the onset of gastrulation uncouples poly(A)-tail length and TE in Drosophila,
571 mirroring the developmental timing of the same uncoupling in zebrafish and Xenopus
572 embryos. The uncoupling of TE from poly(A)-tail length is thus a broadly conserved
573 developmental switch in the nature of translational control, occurring around the onset of
574 gastrulation in both vertebrate and invertebrate embryos.

575 Changing the length of a poly(A) tail would influence both the number of poly(A)-
576 binding proteins (PABPs) that could bind the tail and the probability that at least one
577 PABP would be bound, with the former being more relevant in conditions of saturating
578 PABP and the latter being more relevant in conditions in which tails are competing for
579 PABP. If the number of PABPs that bind the tail were most relevant, then TE changes
580 might have correlated better with absolute tail-length changes than with relative tail-
581 length changes. However, repeating our analyses using absolute tail-length changes
582 rather than \log_2 tail-length fold changes yielded the same results for the respective

583 comparisons, with nearly identical R_s values (Figure 7—figure supplement 2), suggesting
584 that PABP is limiting in the developmental stages in which tail length and TE are coupled,
585 such that mRNAs are competing for PABP.

586 We presume that the correlation between poly(A)-tail length and TE that we observed
587 in oocytes and pre-gastrulation embryos reflects a causal relationship, i.e., that changes in
588 poly(A)-tail length at least partially cause the corresponding changes in TE. The other
589 possibilities are that changes in TE cause changes in tail length or that these two
590 measurements merely correlate without having a causal relationship. Because previous
591 single-gene studies clearly demonstrate a causal role for cytoplasmic polyadenylation,
592 and poly(A)-tail length itself, in regulating the translation of mRNAs during these
593 developmental times (McGrew et al., 1989; Salles et al., 1994; Barkoff et al., 1998), we
594 interpret our observation of a global correlation between poly(A)-tail length and TE as
595 reflecting a causal relationship between the two wherein tail-length changes cause TE
596 changes. Given this interpretation, our results indicate that widespread changes in
597 poly(A)-tail length broadly reshape the translational profiles of oocytes and early
598 embryos.

599 Despite this strong qualitative conclusion, we cannot provide quantitative estimates of
600 the proportion of each TE change that is attributable to each tail-length change, as
601 additional translational regulatory mechanisms presumably act to reinforce or oppose the
602 effects of tail-length-dependent translational regulation. Indeed, we suspect that tail-
603 length-independent processes often act concordantly with tail-length-dependent
604 processes and thereby amplify the apparent effects of tail-length changes. Such
605 amplification explains why some mRNAs, including *cyclin B*, *cyclin B3*, *fuzzy*, *zelda*,

606 *stat92E*, *bicoid*, and *torso*, undergo translational activation that seems out of proportion
607 to their tail-length changes.

608 A primary motivation for using Drosophila in our study was the opportunity to
609 examine the impact of Wispy, PNG, and SMG on poly(A)-tail length and TE. Of
610 particular interest was Wispy, the cytoplasmic poly(A) polymerase that acts during late
611 oogenesis and early embryogenesis, and is essential for the OET (Benoit et al., 2008; Cui
612 et al., 2008). Analysis of *wispy* mutants revealed key insights into both the mechanism of
613 translational activation and the importance of tail shortening (as opposed to tail
614 lengthening) in specifying translational control in Drosophila maturing oocytes and early
615 embryos. Although poly(A)-tail lengths were typically shorter in *wispy*-mutant stage 13
616 oocytes and laid eggs compared to the corresponding wild-type samples, tail length and
617 TE were coupled in both of these *wispy*-mutant contexts, and the relative changes in
618 poly(A)-tail lengths during the OET in wild-type samples were largely preserved in the
619 *wispy*-mutant samples, as were the changes in TE. Thus, the act of cytoplasmic
620 polyadenylation is not necessary for the coupling of poly(A)-tail length to translation.
621 Moreover, cytoplasmic polyadenylation is largely dispensable for specifying which
622 mRNAs are to be translationally activated or repressed, implying that in Drosophila,
623 selective deadenylation is more important for imparting this specificity. This greater
624 importance for deadenylation does not preclude a role for selective cytoplasmic
625 polyadenylation in translational control in Drosophila—differences were observed when
626 comparing TE changes in wild-type and *wispy*-mutant samples (Figure 5D), and when
627 comparing RPF measurements between wild-type and *wispy*-mutant samples (Figure 5—
628 figure supplement 1D), including for *cortex*, a critical OET regulator. However, the

629 greater importance of selective deadenylation for specifying translational control in
630 Drosophila differs from the prevailing paradigm of vertebrates, which centers on
631 selective cytoplasmic polyadenylation of mRNAs with cytoplasmic polyadenylation
632 elements (Pique et al., 2008; Weill et al., 2012). This suggests either a fundamental
633 difference between invertebrates and vertebrates or that an underappreciated component
634 of translational control in vertebrates occurs through more global cytoplasmic
635 polyadenylation with selective deadenylation.

636 Despite the surprisingly modest perturbation of translational regulation that we
637 observed in *wispy*-mutant laid eggs during egg activation, these laid eggs are blocked at
638 the OET because of defective progression through meiosis and failure of pronuclei to
639 fuse (Benoit et al., 2008; Cui et al., 2008). Why does this developmental arrest occur if
640 translational regulation is largely preserved during egg activation in *wispy* mutants? One
641 possibility is that the absolute level of translation in *wispy*-mutant eggs is reduced such
642 that they make an inadequate amount of one or more essential protein. The other
643 possibility rests on the observation that although TE changes and RPFs were remarkably
644 concordant in the *wispy*-mutant and wild-type samples, they were not identical, and thus
645 an aberrant change in expression for one or more key factor, such as *cortex*, might be
646 sufficient to trigger the developmental arrest of *wispy*-mutant laid eggs.

647 Activity of the PNG kinase during egg activation affects most mRNAs that undergo
648 translational activity changes at this developmental transition, both those that are up- and
649 downregulated (Kronja et al., 2014b). Although the direct targets of PNG kinase remain
650 to be identified, PNG is required to relieve the repressive effects of PUM (Vardy and Orr-
651 Weaver, 2007a) and thereby derepresses translation of *smg* and other mRNAs (Tadros et

652 al., 2007). In wild-type activated eggs the mRNAs dependent on PNG for translational
653 up- or downregulation exhibited corresponding increases or decreases in poly(A)-tail
654 length, and these tail-length changes did not occur in *png* mutants. Thus, for both
655 translationally activated and translationally repressed mRNAs, the downstream effectors
656 of PNG appear to regulate translation primarily through changes in poly(A)-tail length.

657 Translational repressors in addition to SMG have been proposed to contribute to
658 PNG-dependent regulation (Tadros et al., 2007). Our results are consistent with the idea
659 that PNG activates at least one additional translational repressor, as the set of mRNAs
660 dependent on PNG for their translational downregulation were still somewhat
661 translationally repressed and deadenylated relative to all other mRNAs in *smg*-mutant
662 embryos, although less than in wild-type embryos. Additionally, although SMG is
663 reported to act partly through a mechanism that does not involve deadenylation (Nelson
664 et al., 2004; Semotok et al., 2005), essentially all the derepression observed in the *smg*-
665 mutant embryos was accompanied by tail-length increases. Perhaps at other times SMG
666 causes direct translational repression, but in 0–1 h embryos it seems to act predominantly
667 through deadenylation.

668 Within the overall framework in which tail-length changes cause the up- or
669 downregulation of mRNAs for a vast repertoire of different genes, we discovered
670 unanticipated complexities and exceptions. One unanticipated complexity was the
671 evidence for tail-length-independent processes that appear to amplify the tail-length-
672 dependent effects, as already discussed. Additional unanticipated complexity was
673 observed during oocyte maturation, in which surprisingly diverse patterns of regulatory
674 dynamics produce the ultimate changes in TE. Single-gene studies in Xenopus, which

675 show that *c-mos* mRNA becomes polyadenylated and translated prior to the mRNAs for
676 several *cyclin B* genes (Richter, 2007; Pique et al., 2008), hint that the complex landscape
677 of translational control observed in *Drosophila* extends to vertebrate oocyte maturation.
678 The diverse temporal behaviors of translational regulation during oocyte maturation
679 might reflect the evolving demands on the maturing oocyte, or perhaps simply
680 differences in the timing of expression of RNA-binding proteins that interact with these
681 different sets of mRNAs. Regardless, the observation of different temporal patterns of
682 regulation indicates that rather than a being a sudden switch, oocyte maturation in
683 *Drosophila* is a progressive process, whereby mRNAs are translationally activated or
684 repressed at different times throughout this developmental transition.

685 Another surprise was the identification of a set of mRNAs for which tail-length
686 changes did not correspond to TE changes during oocyte maturation. This exception to
687 the general pattern occurred for the mRNAs that had undergone deadenylation between
688 oocyte stages 13 and 14 yet not only remained stable but also continued to be translated
689 with relatively high efficiency (Figure 2—figure supplement 2). To escape the general
690 regulatory environment of the cytoplasm, these mRNAs might exploit unique interactions
691 with the translational machinery analogous to the translational activation of histone
692 mRNAs through stem-loop binding protein (Cakmakci et al., 2008), or they might
693 localize to a subcellular compartment that lacks coupling. The deadenylation of these
694 mRNAs during oogenesis might prime them for rapid degradation during embryogenesis.
695 Most mRNAs from genes encoding proteasome subunits fell into this class. Previous
696 comparisons of the proteome and translation changes suggest that extensive proteolysis
697 occurs at egg activation (Kronja et al., 2014b). Upregulation of the proteasome in late

698 oogenesis might necessitate a mechanism to downregulate it rapidly during
699 embryogenesis, perhaps facilitated by pre-deadenylating the corresponding mRNAs
700 before egg activation.

701 The molecular mechanism that couples TE with poly(A)-tail length is unknown, as is
702 the mechanism of the uncoupling that occurs at gastrulation. Nevertheless, our results,
703 which show that widespread changes in poly(A)-tail length broadly reshape translational
704 activity during oocyte and embryo development, demonstrate the importance of this
705 coupling mechanism and provide a resource that documents the thousands of affected
706 genes with information on the timing, magnitude, and inferred consequences of the tail-
707 length changes for mRNAs from each of these genes. Moreover, the identification of
708 unanticipated complexities and exceptions reveals the rich posttranscriptional regulatory
709 landscape of oocytes and early embryos and points to additional mechanisms that operate
710 for some mRNAs in specific settings, which can now be targeted for investigation.

711

712 **ACKNOWLEDGEMENTS**

713 We thank Mariana Wolfner for providing stocks, the Whitehead Genome Sequencing
714 Core for sequencing, and Anthony Mahowald for comments on the manuscript. This
715 work was supported by NIH grants GM39341 and GM118098 (T.L.O.-W.) and
716 GM067031 (D.P.B.). A.O.S. was supported by NIH Medical Scientist Training Program
717 fellowship T32GM007753, and I.K. was supported by the Feodor Lynen Postdoctoral
718 Fellowship from the Alexander von Humboldt Foundation. T.L.O.-W. is an American
719 Cancer Society Research Professor, and D.P.B. is an investigator of the Howard Hughes
720 Medical Institute.

721

722 **MATERIALS AND METHODS**723 **Drosophila Stocks**

724 All flies were kept at 18, 22 or 25 °C according to standard procedure (Greenspan,
725 1997). *Oregon R* flies were used as a wild-type control. The null *png*¹⁰⁵⁸ allele was
726 previously described (Shamanski and Orr-Weaver, 1991; Fenger et al., 2000). The
727 *wispy* hemizygote mutants were derived from a cross between *wisp*⁴¹/*FM6* (Cui et
728 al., 2008) (kindly provided by Mariana Wolfner, Cornell) and *Df(1)RA47/FM7c*
729 flies (BL961, obtained from the Bloomington Drosophila Stock Center). The
730 *smaug* hemizygote mutants resulted from a cross between *smg*¹/*TM3, Sb[1]*
731 (BL5930, obtained from the Bloomington Drosophila Stock Center) and *Df(3L)Scf-*
732 *R6, Diap1[1] st[1] cu[1] sr[1] e[s] ca[1]/TM3, Sb[1]* flies (BL4500, obtained from
733 the Bloomington Drosophila Stock Center). Unfertilized eggs were collected from
734 crosses to *twine*^{HB5} mutant males, which fail to make sperm (Courtot et al., 1992).

735

736 **Oocyte and Embryo collection**

737 Egg chambers were hand-dissected in Grace's Unsupplemented Insect Media (Gibco)
738 from three-day old flies that had been fattened for two days with wet yeast at 22 °C.
739 Approximately 300 egg chambers were collected per oogenesis stage. Oocyte stages 11
740 through 14 were distinguished using morphological criteria (Spradling, 1993). Activated
741 eggs were collected as previously described (Kronja et al., 2014b). Samples were
742 transferred to RPF lysis buffer (10 mM Tris-HCl, pH 7.4, 5 mM MgCl₂, 100 mM KCl, 2
743 mM DTT, 100 µg ml⁻¹ cycloheximide, 1% Triton X-100, 500 U ml⁻¹ RNasin Plus, and

744 protease inhibitor (1x complete, EDTA-free, Roche); wild-type stage 14 oocyte and
745 activated egg samples were transferred to RPF lysis buffer lacking cycloheximide),
746 centrifuged at 10000 rpm for 5 min, and the supernatants were collected and flash frozen
747 in liquid nitrogen to be stored at -80 °C. Ultimately, the yield was approximately 40-50
748 µg of total RNA in 70-120 µl lysate.

749 Embryos were collected at 25 °C by discarding two initial one-hour collections to
750 avoid collecting embryos held within females for prolonged time. Only the subsequent
751 0–1 h collection was then processed for sequencing analysis. The same embryo
752 collection strategy was applied to *smg* or *wispy* mutants, though for the *wispy* mutant the
753 collection was extended to 0–2 h as one hour was too short to gather a sufficient number
754 of laid eggs for sequencing. To obtain *OrR* 2–3 h, 3–4 h and 5–6 h embryo samples, 0–1
755 h embryos (collected after two previous one-hour collections were discarded) were
756 incubated in a “humid chamber” at 25 °C for additional 2, 3 or 5 h, respectively.

757

758 **Embryo Staging**

759 Drosophila females can hold developing embryos or lay unfertilized eggs, and so to
760 ensure that the vast majority of the embryos processed for downstream analyses were in
761 the expected developmental stage, a fraction of each embryo collection (approximately
762 10-20%) was stained with DAPI. This approach was also used to confirm that the
763 embryos laid by mutant mothers (*png*, *smg*, or *wispy*) were developmentally arrested as
764 previously described. Briefly, collected embryos were dechorionated in 50% bleach for 3
765 min at room temperature, extensively washed with water, dried and then transferred into
766 a scintillation vial that contained methanol. To remove the vitelline membrane from the

767 embryos, an equal volume of heptane was added and the vial was vigorously shaken by
768 hand for 2 min. Next, embryos were fixed overnight in methanol at 4 °C. Embryos were
769 then sequentially rehydrated in a mix of methanol:PBS (9:1, 3:1, 1:1, 1:3) for at least 5
770 min per step. After a wash in PBS, embryos were incubated for 15 min in a 1 µg ml⁻¹
771 solution of DAPI in PBS, followed by 30 min wash in PBS containing 0.1% Triton X-
772 100. Finally, after removing all the washing solution, samples were mounted in
773 Vectashield.

774

775 **Transcript Models**

776 Reference transcript annotations were downloaded from the UCSC Genome browser
777 (dm6 in refFlat format), and for each gene the longest transcript was chosen as the initial
778 representative transcript model. Non-coding genes and overlapping genes on the same
779 strand were removed from this analysis. PAL-seq tags from all wild-type samples were
780 combined, filtered to remove tags with a poly(A) tail <20 nt, and then aligned with STAR
781 (Dobin et al., 2013). 3' UTRs were annotated by identifying positions where ≥2 PAL-seq
782 tags aligned at the same position between the stop codon of one gene and the
783 transcription start site of the neighboring gene on the same strand. Isoforms were
784 annotated as described previously (Jan et al., 2011), using a 60 nt window and a
785 maximum 3'-UTR length of 4100 nt. If a new 3' terminus was annotated that was distal to
786 the initial model, the 3' end of the model was extended to the distal isoform. If not, the
787 initial representative transcript model was used. The resulting set of representative
788 transcript models (referred to as “mRNAs”) used for our analyses is available at
789 <http://www.ncbi.nlm.nih.gov/geo> under accession number GSE83616. Models for which

790 the selected 3'-end isoform (either the initial refFlat 3' end or an extension based on our
791 re-annotation) overlapped with a snoRNA or snRNA were included in the analysis of
792 sequencing data but excluded from figures.

793

794 **Ribosome Footprint Profiling, RNA-seq, and PAL-seq**

795 Samples were split and prepared for ribosome-footprint profiling and RNA-seq as
796 described (Kronja et al., 2014b), as well as for PAL-seq as described (Subtelny et al.,
797 2014). Detailed protocols are available at <http://bartellab.wi.mit.edu/protocols.html>. The
798 wild-type stage 14 oocyte and activated egg samples were prepared using RPF lysis
799 buffer and sucrose gradients that did not contain cycloheximide, all other samples were
800 prepared using RPF lysis buffer and sucrose gradients that contained cycloheximide.
801 Because TE changes between wild-type stage 14 oocytes and activated eggs for samples
802 prepared with and without cycloheximide correlated very well (Kronja et al., 2014b), the
803 omission of cycloheximide did not affect our observations pertaining to these stages.
804 RPF and RNA-seq reads were mapped to ORFs of representative transcript models as
805 described, which excluded the first 50 nt of each ORF to eliminate signal from ribosomes
806 that initiated after adding cycloheximide (Subtelny et al., 2014). PAL-seq tags were
807 mapped to 3' UTRs of representative transcript models, and PAL-seq fluorescence
808 intensities were converted to tail lengths as described (Subtelny et al., 2014).

809

810 **Clustering TE dynamics**

811 TE values (\log_2) for stage 11, 12, 13, and 14 oocytes, or for stage 14 oocytes, 0–1 h
812 embryos, and 2–3 h embryos were normalized by the median TE value for the mRNAs in

813 the corresponding sample from Figure 2 or Figure 1B, respectively, and were then
814 entered into the Short Time-series Expression Miner (STEM) (Ernst and Bar-Joseph,
815 2006), which normalized the data relative to the first sample and then used the STEM
816 clustering method to identify significantly enriched profiles (p value < 0.05, following
817 Bonferroni correction). The default settings were used, except a maximum unit change
818 of one in model profiles was allowed between time points, and only mRNAs with ≥ 0.5 or
819 $\leq -0.5 \log_2$ fold change between any two samples were placed in a cluster. A heatmap of
820 all expression patterns was generated in Matlab using the normalized data.

821

822 Sequencing data

823 The RNA-seq and ribosome-footprint profiling data for wild-type stage 14 oocytes and
824 activated eggs, and *png*-mutant activated eggs were previously published (Kronja et al.,
825 2014b) and were reanalyzed for this study. The raw data for these previously published
826 datasets are available at the Gene Expression Omnibus
827 (<http://www.ncbi.nlm.nih.gov/geo>) under accession number GSE52799, and the
828 processed data files used for this study are under accession number GSE83616. The PAL-
829 seq data for those samples had not been published and are available along with all of the
830 other RNA-seq, ribosome profiling, and PAL-seq data and processed data files under
831 accession number GSE83616. All of the processed data are also available in
832 Supplementary File 2.

833

834 Statistical analysis

835 Unless noted otherwise, all correlations report the Spearman correlation coefficient, and
836 all statistical tests were two-sided. Comparing the TE changes observed between
837 biological replicates for wild-type stage 14 oocytes and activated eggs correlated very
838 well ($R_s = 0.94$) (Kronja et al., 2014b), even though cycloheximide was omitted from one
839 of the replicates. Likewise, TE of activated egg highly correlated with that of 0–1 h
840 embryo ($R_s = 0.88$). Although we did not analyze replicates of PAL-seq measurements in
841 the current study, previous analysis of biological replicates demonstrate the
842 reproducibility mean tail lengths measured using this technique ($R_s = 0.83$). Similar
843 correlations were observed in the current study when comparing stages for which little if
844 any differences in tail lengths were expected, including activated egg and 0–1 h embryo
845 ($R_s = 0.86$), stage 11 and stage 12 oocyte ($R_s = 0.94$), stage 12 and stage 13 oocyte ($R_s =$
846 0.88), as well as *png* and wild-type oocytes at stage 14 ($R_s = 0.86$), which was prior to
847 PNG activation (Supplementary File 1 and Figure 6—figure supplement 1A).
848

849 **Figure 1. Transient coupling between poly(A)-tail length and translational
850 efficiency in embryos.**

851 (A) Time line of the developmental transitions probed in this study, illustrating the
852 presence of maternal and zygotic mRNAs (pink and purple, respectively). (B)
853 Relationship between mean poly(A)-tail length and relative translational efficiency (TE)
854 at the indicated developmental stage (*top*), and the relationship between tail-length and
855 TE changes observed between adjacent stages (*bottom*). For each stage, tail-length and
856 TE measurements were from the same sample. In the top panels, results are plotted for
857 all mRNAs that had ≥ 100 poly(A)-tail length measurements (tags), ≥ 10.0 reads per
858 million mapped reads (RPM) in the RNA-seq data, and >0 RPM in the ribosome-
859 profiling data. In each sample, TE values (\log_2) were median centered by subtracting the
860 median TE value of that sample from each value (median values in stage 14 oocytes, 0–1
861 h embryos, 2–3 h embryos, 3–4 h embryos, and 5–6 h embryos were –0.2523, –0.1329,
862 0.4799, 0.6469, and 0.6447, respectively). In the bottom panels, results are plotted for all
863 mRNAs that had ≥ 100 poly(A) tags and ≥ 10.0 RPM in the RNA-seq data of both samples,
864 and ≥ 10.0 RPM in the ribosome-profiling data of one of the two samples and >0 RPM in
865 the other. TE fold-change values (\log_2) were median centered for each comparison
866 (median values, 0.2027, –0.0047, 0.0701, and –0.003 from left to right). The Spearman
867 correlation coefficient (R_s) and number of mRNAs (n) are shown in each plot. The TE
868 data for stage 14 were from Kronja et al. (2014b). (C) Abundance and TE of *zelda*,
869 *stat92E*, *smaug*, and *bicoid* mRNA at the indicated developmental stages (RPKM is reads
870 per kilobase per million mapped reads). TE values (\log_2) for each stage were median
871 centered as described above, using the median values (\log_2) reported in the legends of

872 Figure 1B and Figure 2. The data for stage 14 were from Kronja et al. (2014b). If no
873 RPF reads were observed in a sample, TEs were calculated using a pseudocount of 1 read.
874 Points for which TE is based on either a single read or pseudocount are in grey, as are the
875 lines connecting to them. Other TEs were based on ≥ 25 RPF reads, except the TEs for
876 *bicoid* in stage 14 oocytes and 3–4 h embryos (3 and 9, respectively) and the TE for
877 *smaug* in stage 13 oocytes (11 reads).

878

879 **Figure 2. Coupling between poly(A)-tail length and translational efficiency in**
880 **oocytes.**

881 Relationship between mean poly(A)-tail length and TE in either oocytes at the indicated
882 stage or activated eggs (*top*), and the relationship between tail-length and TE changes
883 observed between adjacent stages (*bottom*). TE values (\log_2) were median centered
884 (median values in stage 11, 12, 13, and 14 oocytes and activated eggs were -0.6641 , $-$
885 0.9006 , -1.38 , -0.2523 , and -0.0158 , respectively). TE fold-change values (\log_2) were
886 median centered for each comparison (median values, -0.1961 , -0.3969 , 1.0886 , and
887 0.2123 from left to right). The TE data for stage 14 oocytes and activated eggs were
888 from Kronja et al. (2014b), and the plot of mean poly(A)-tail length and TE for the stage
889 14 oocyte is modified from Figure 1B. Otherwise, these panels are as in Figure 1B.

890

891 **Figure 3. Dynamics of translational regulation during oocyte maturation.**

892 (A) Distinct patterns of TE changes during oocyte maturation. TE values (\log_2) for
893 mRNAs in oocytes from stages 11 through 14 that had ≥ 10.0 RPM in the RNA-seq data
894 for all samples, and ≥ 10.0 RPM in the ribosome-profiling data for at least one sample and

895 >0.0 RPM in the others were median centered as in Figure 2. The median-centered TEs
896 for stage 12, 13, and 14 oocytes were normalized to those of stage 11 oocytes and then
897 clustered into defined patterns. The heatmap shows clustered TE changes for all mRNAs
898 with ≥ 0.5 or ≤ -0.5 \log_2 fold change between any two samples. Clusters are identified by
899 number, and stylized graphs illustrate the TE dynamics of sample clusters. Clusters that
900 are significantly overrepresented are marked with an asterisk (p value < 0.05 , following
901 Bonferroni correction). **(B)** Changes in TE (black) and mean poly(A)-tail length (green)
902 of *cyclin B* mRNA during oocyte maturation. TEs (\log_2) were normalized as in Figure 3A,
903 and the median of the changes in mean poly(A)-tail length (\log_2) for all mRNAs over
904 these stages is shown as a grey line. Fold changes (\log_2) calculated relative to stage 11
905 oocytes are indicated on the respective y axes.

906

907 **Figure 4. TEs and Poly(A) tail lengths of selected cell-cycle regulators during oocyte
908 maturation.**

909 **(A)** Relationship between net tail-length and TE changes observed after oocyte
910 maturation, highlighting the behavior of *cyclin B*, *cyclin B3*, and *fizzy*. The TE data for
911 stage 14 oocytes were from Kronja et al. (2014b). Values from stage 14 oocytes are
912 compared to those of stage 11 oocytes (median value used for median centering, 0.389);
913 otherwise, as in Figure 1B. **(B)** Distributions of poly(A)-tail lengths of mRNAs from
914 *cyclin B* (left), *cyclin B3* (middle), and *fizzy* (right) at the indicated developmental stages.
915 Mean poly(A)-tail lengths are in parentheses. **(C)** Relationship between tail-length and
916 TE changes observed after egg activation, plotting the same points as in Figure 2 (bottom
917 right), but highlighting the behavior of *Toll*, *bicoid*, and *torso*. **(D)** Distributions of

918 poly(A)-tail lengths of mRNAs from *Toll* (*left*), *bicoid* (*middle*), and *torso* (*right*) at the
919 indicated developmental stages; otherwise, as in Figure 4B.

920

921 **Figure 5. Widespread impact of Wispy on poly(A)-tail lengths but not TE.**

922 (A) Comparison of mean poly(A)-tail lengths in wild-type and *wispy*-mutant stage 13
923 oocytes (*left*) and in wild-type cleavage-stage embryos and *wispy*-mutant laid eggs (*right*).
924 Plotted are mean poly(A)-tail lengths of mRNAs with ≥ 100 poly(A) tags in both the wild-
925 type and *wispy*-mutant sample at the indicated developmental stage. mRNAs that had
926 mean tail-length values ≤ 4 nt are reported as 4 nt. The dashed line is for $y = x$. (B)
927 Relationship between mean poly(A)-tail length and TE at the indicated developmental
928 stage in *wispy*-mutant oocytes (*left*) and laid eggs (*right*). The TEs were calculated by
929 dividing *wispy*-mutant stage 13 oocyte or laid egg RPF data by wild-type stage 13 oocyte
930 or 0–1 h embryo RNA-seq data, respectively. TE values (\log_2) were median centered
931 (median values in *wispy*-mutant stage 13 oocytes and laid eggs, -1.0551 and 0.3302,
932 respectively). mRNAs that had mean tail-length values ≤ 4 nt are reported as ≤ 4 nt;
933 otherwise, as in Figure 1B. (C) Relationship between tail-length and TE changes
934 observed between *wispy*-mutant laid eggs and stage 13 oocytes. TE fold-change values
935 (\log_2) were median centered (median value, 0.8132); otherwise, as in Figure 1B. The
936 mRNAs that seemed to have increased poly(A)-tail length over this time tended to have
937 very short poly(A)-tails in stage 13 oocytes, suggesting that their positive fold-change
938 values reflected difficulties in accurately measuring poly(A)-tails < 8 nt using PAL-seq
939 rather than genuine increases in poly(A)-tail length. (D) Comparison of TE changes for
940 wild-type and *wispy*-mutant samples during the OET (*left*) and comparison of tail-length

941 changes for wild-type and *wispy*-mutant samples during the OET (*right*). TE fold-change
942 values (\log_2) were median centered (median values for the wild-type and *wispy*-mutant
943 samples, 0.7207 and 0.8367, respectively). Dashed line is for $y = x$. Otherwise, this panel
944 is as in Figure 1B.

945

946 **Figure 6. Widespread translational regulation by PAN GU mediated primarily by**
947 **changes in poly(A)-tail length.**

948 (A) Relationship between the TE changes in wild-type activated eggs relative to wild-
949 type stage 14 oocytes and in wild-type activated eggs relative to *png*-mutant activated
950 eggs. TE fold-change values (\log_2) were median centered (median values for wild-type
951 activated egg relative to stage 14 oocyte and for wild-type activated egg relative to *png*-
952 mutant activated egg, 0.3065 and 0.0881, respectively). Results are plotted for all
953 mRNAs that had ≥ 10.0 RPM in the RNA-seq data of all samples, and ≥ 10.0 RPM in the
954 ribosome profiling data of at least one of the two samples being compared and >0.0 RPM
955 in the other. mRNAs ≥ 4 -fold up- or downregulated in both comparisons were defined as
956 the PNG-dependent up- or downregulated mRNAs, respectively. The TE data for wild-
957 type stage 14 oocytes and activated eggs and *png*-mutant activated eggs were from
958 Kronja et al. (2014b). Dashed line is for $y = x$. (B) Relationship between mean tail-
959 length changes and TE changes after egg activation for wild-type activated eggs (*left*;
960 modified from Figure 2) and *png*-mutant activated eggs (*right*). The mRNAs with PNG-
961 dependent downregulation are highlighted in red (Supplementary File 3), analyzing and
962 highlighting the same mRNAs in both plots. TE fold-change values (\log_2) were median
963 centered (median for wild-type and *png*-mutant samples, 0.1366 and 0.6448, respectively).

964 Black lines indicate median values for all mRNAs, and red lines indicate median values
965 for the PNG-dependent downregulated mRNAs. The TE data for wild-type stage 14
966 oocytes and activated eggs and *png*-mutant activated eggs are from Kronja et al. (2014b).
967 Otherwise, this panel is as in Figure 1B. **(C)** The plots of panel **B**, highlighting the PNG-
968 dependent upregulated mRNAs in blue (Supplementary File 3). **(D)** Relationship
969 between tail-length and TE changes during egg activation in wild-type relative to the
970 *png*-mutant samples, analyzing and highlighting the same mRNAs as in panels **B** and **C**.
971 TE fold-change values (\log_2) were median centered (median value, -0.727). Otherwise,
972 this panel is as in Figure 6B.

973

974 **Figure 7. Translational regulation by Smaug mediated primarily by changes in**
975 **poly(A)-tail length.**

976 **(A)** Relationship between mean tail-length changes and TE changes during the OET for
977 wild-type 0–1 h embryos (*left*) and *smg*-mutant 0–1 h embryos (*right*), comparing wild-
978 type or *smg*-mutant 0–1 h embryos to wild-type stage 14 oocytes. The wild-type plot is
979 redrawn from Figure 1B, but includes only the mRNAs that also passed the cutoffs for
980 the *smg*-mutant comparison. TE fold-change values (\log_2) were median centered (median
981 for the wild-type and *smg*-mutant samples, 0.175 and -0.0221, respectively). The PNG-
982 dependent downregulated mRNAs are in red (Supplementary File 3), analyzing and
983 highlighting the same mRNAs in both plots. Otherwise, this panel is as in Figure 6B.
984 **(B)** The plots of panel **A**, highlighting the PNG-dependent upregulated mRNAs in blue
985 (Supplementary File 3). **(C)** Relationship between tail-length and TE changes for wild-
986 type 0–1 h embryos relative to *smg*-mutant 0–1 h embryos, analyzing and highlighting

987 the same mRNAs as in panel A. TE fold-change values (\log_2) were median centered
988 (median value, 0.2634). Otherwise, this panel is as in Figure 6D.

989

990 **Figure 1—figure supplement 1. Dynamics of translational regulation during the
991 OET and early embryonic development.**

992 Distinct patterns of TE changes during the OET and early embryonic development. TE
993 values (\log_2) for mRNAs in stage 14 oocytes, 0–1 h embryos, and 2–3 h embryos that had
994 ≥ 10.0 RPM in the RNA-seq data for all samples, and ≥ 10.0 RPM in the ribosome-
995 profiling data for at least one sample and >0.0 RPM in the others were median centered
996 as in Figure 1B. The median-centered TEs for 0–1 h embryos and 2–3 h embryos were
997 normalized to those of stage 14 oocytes and then clustered into defined patterns. Clusters
998 are identified by number, and stylized graphs illustrate the TE dynamics of each cluster.
999 Clusters that were significantly overrepresented are marked with an asterisk (p value
1000 <0.05 , following Bonferroni correction); otherwise, as in Figure 3.

1001

1002 **Figure 2—figure supplement 1. Widespread translational regulation during oocyte
1003 maturation.**

1004 (A) Relationship between TEs in stage 11 and stage 14 oocytes. TE values (\log_2) were
1005 median centered (median values in stage 11 and stage 14 oocytes, -0.5153 and -0.1318 ,
1006 respectively). Results are plotted for all mRNAs that had ≥ 10.0 RPM in the RNA-seq
1007 data of both samples and ≥ 10.0 RPM in the ribosome profiling data of at least one of the
1008 two samples and >0.0 RPM in the other. The median-centered TE fold-change values
1009 (\log_2) of stage 14 relative to stage 11 (median, 0.0147) were used to identify mRNAs that
1010 were ≥ 2 -fold up- or downregulated in stage 14 oocytes, which are highlighted in red and
1011 blue, respectively; otherwise as in Figure 1B. (B) Relationship between the change in
1012 protein level (Kronja et al., 2014a) and change in TE observed after oocyte maturation.

1013 TE and protein fold-change (\log_2) values were median centered (median values of 0.1236
1014 and 0.0474, respectively). Results are plotted for all mRNAs that had ≥ 10.0 RPM in the
1015 RNA-seq data, ≥ 10.0 RPM in the ribosome profiling of one of the two samples and > 0.0
1016 RPM in the other, and proteins with ≥ 2 unique peptides in each of three independent
1017 mass spectrometry experiments. **(C)** Relationship between tail-length and TE changes
1018 observed after oocyte maturation, redrawn from Figure 4A, but highlighting points for
1019 mRNAs with a TE ≤ 0.1 in stage 11 oocytes in blue (Supplementary File 3) and those for
1020 *cyclin B*, *cyclin B3*, and *fizzy* in yellow, green, and purple, respectively. The dashed line
1021 indicates a TE increase of 10 fold.

1022

1023 **Figure 2—figure supplement 2. Uncoupled behavior observed for a subset of**
1024 **mRNAs between the last stages of oocyte maturation.**

1025 **(A)** The relationship between the tail-length and TE changes observed between stage 14
1026 oocytes relative to stage 13 oocytes, redrawn from Figure 2, highlighting in blue mRNAs
1027 that had tail-length decreases of at least 29% (\log_2 fold change of -0.5), and in red
1028 mRNAs encoding proteasome subunits (Supplementary File 3). **(B)** The relationship
1029 between tail length and TE observed in stage 13 and 14 oocytes (*left* and *right*,
1030 respectively) analyzed as in Figure 2 but plotting results for only the mRNAs examined
1031 in panel **A** and highlighting the same sets of mRNAs as in panel **A**. TE values (\log_2) were
1032 median centered (median values for stage 13 and 14 oocytes, -1.2409 and -0.0779 ,
1033 respectively).

1034

1035 **Figure 5—figure supplement 1. Impact of Wispy on the poly(A)-tail length of most**
1036 **mRNAs, which biased mRNA recovery during poly(A) selection.**

1037 (A) The plots from Figure 5A, highlighting mRNAs encoding ribosomal proteins in red
1038 (Supplementary File 3). (B) Relationship between mean poly(A)-tail length and TE at
1039 the indicated developmental stage in *wispy*-mutant samples. The TEs were calculated
1040 using *wispy*-mutant RNA-seq and ribosome profiling data, and are median centered
1041 (median values in stage 13 oocytes and laid eggs, -0.5729 and 0.5761, respectively);
1042 otherwise, as in Figure 5B. (C) Relationship between measured RNA abundance and
1043 poly(A)-tail length in wild-type stage 13 oocytes and 0–1 h embryos, and in *wispy*-mutant
1044 stage 13 oocytes and laid eggs. Results are plotted for mRNAs that had ≥ 100 poly(A)
1045 tags in both the wild-type and *wispy*-mutant samples for the corresponding stage and
1046 ≥ 10.0 RPM in the RNA-seq data in the wild-type sample. The same mRNAs are plotted
1047 in corresponding wild-type and *wispy*-mutant samples. mRNAs that had mean tail-length
1048 values ≤ 4 nt are reported as ≤ 4 nt. (D) Comparison of RPF measurements for wild-type
1049 and *wispy*-mutant stage 13 oocytes (*left*) and cleavage-stage embryos (*right*). Results are
1050 plotted for all mRNAs with ≥ 10.0 RPM in the ribosome-profiling data of either the wild-
1051 type or *wispy*-mutant sample, and any mRNA with 0 reads in either sample was given a
1052 pseudocount of 1 read and highlighted in blue or purple (Supplementary File 3).

1053

1054 **Figure 6—figure supplement 1. Perturbation of tail-length and TE during the**
1055 **oocyte-to-embryo transition in *png*-mutant samples.**

1056 (A) Comparison of mean poly(A)-tail lengths and TEs between wild-type and *png*-mutant
1057 stage 14 oocytes, and between wild-type and *png*-mutant activated eggs. TE values

1058 (log₂) were median centered (median values in wild-type and *png*-mutant stage 14
1059 oocytes, -0.2182 and -1.182, respectively, and wild-type and *png*-mutant activated eggs
1060 0.0724 and -0.2394, respectively. Results are plotted for mRNAs that had ≥100 poly(A)
1061 tags, ≥10.0 RPM in the RNA-seq data, and >0 RPM in the ribosome profiling data for
1062 each sample. **(B)** Comparison of mean poly(A)-tail lengths and TEs between *png*-mutant
1063 stage 14 oocytes and activated eggs, and between wild-type stage 14 oocytes and
1064 activated eggs; otherwise, as in panel **A**.

1065

1066 **Figure 7—figure supplement 1. Smaug-dependent translational repression of**
1067 **Smaug binding targets, mediated primarily by changes in poly(A)-tail length.**
1068 Shown is the relationship between mean tail-length changes and TE changes during the
1069 OET for wild-type and *smg*-mutant 0–1 h embryos (*left* and *right*, respectively),
1070 highlighting mRNAs previously reported to be bound by SMG in the early embryo (Chen
1071 et al., 2014); otherwise as in Figure 6B.

1072

1073 **Figure 7—figure supplement 2. Relationship between poly(A)-tail length changes**
1074 **and TE changes throughout development, plotting absolute rather than relative tail-**
1075 **length changes.**

1076 Shown are the relationships between the absolute differences in mean tail-length and TE
1077 changes observed between stages; otherwise, as in the corresponding panels from Figures
1078 1, 2, 4, 5, 6, and 7.

1079

1080 **Supplementary File 1. Relationships between RNA-seq, ribosome profiling, and**
1081 **PAL-seq measurements for wild-type samples at different developmental stages.**

1082 The Spearman correlation coefficients for all unique pairwise combinations of stages are
1083 shown. For the RNA-seq or ribosome-profiling comparisons, all mRNAs with ≥ 10.0
1084 RPM in both samples of the respective datasets being compared were included. For the
1085 PAL-seq comparisons, all mRNAs with ≥ 100 poly(A) tags in both samples being
1086 compared were included.

1087

1088 **Supplementary File 2. Processed RNA-seq, ribosome-profiling, and PAL-seq data.**

1089 Each of the 16 spreadsheets of this file reports the data for the indicated sample. Within
1090 each sheet, the initial Refseq ID is the dm6 Refseq ID that was selected for each gene on
1091 the basis of being the longest annotated isoform of that gene. For many genes, the 3' end
1092 of this gene model was extended to include the most distal isoform supported by PAL-seq
1093 data. RPKM is reads per kilobase per million mapped reads. Descriptions of the
1094 analyses include the measurement cutoffs applied to RNA-seq, ribosome profiling, and
1095 PAL-seq data, as applicable. The 8th and 9th columns specify whether a 10 RPM cutoff
1096 for RNA-seq or ribosome profiling data was met, and the 10th column specifies whether a
1097 100 tag cutoff for PAL-seq data was met. All transcripts with a 3' UTR that overlapped a
1098 snoRNA or snRNA were excluded from analysis, as indicated in the final column.

1099

1100 **Supplementary File 3. Lists of mRNAs highlighted in figures.**

1101 This file lists mRNAs that are highlighted in Figures 6 and 7, and Figure 2–figure
1102 supplement 1C, Figure 2–figure supplement 2, Figure 5–figure supplement 1, and Figure
1103 7–figure supplement 1.
1104

1105

REFERENCES

1106

1107 Barckmann, B., and Simonelig, M. (2013). Control of maternal mRNA stability in germ
 1108 cells and early embryos. *Biochim Biophys Acta* *1829*, 714-724.

1109

1110 Barkoff, A., Ballantyne, S., and Wickens, M. (1998). Meiotic maturation in *Xenopus*
 requires polyadenylation of multiple mRNAs. *Embo J* *17*, 3168-3175.

1111

1112 Benoit, B., Mitou, G., Chartier, A., Temme, C., Zaessinger, S., Wahle, E., Busseau, I.,
 1113 and Simonelig, M. (2005). An essential cytoplasmic function for the nuclear
 1114 poly(A) binding protein, PABP2, in poly(A) tail length control and early
 development in *Drosophila*. *Dev Cell* *9*, 511-522.

1115

1116 Benoit, P., Papin, C., Kwak, J.E., Wickens, M., and Simonelig, M. (2008). PAP- and
 1117 GLD-2-type poly(A) polymerases are required sequentially in cytoplasmic
 polyadenylation and oogenesis in *Drosophila*. *Development* *135*, 1969-1979.

1118

1119 Besse, F., and Ephrussi, A. (2008). Translational control of localized mRNAs: restricting
 protein synthesis in space and time. *Nat Rev Mol Cell Biol* *9*, 971-980.

1120

1121 Cakmakci, N.G., Lerner, R.S., Wagner, E.J., Zheng, L., and Marzluff, W.F. (2008).
 1122 SLIP1, a factor required for activation of histone mRNA translation by the stem-
 loop binding protein. *Mol Cell Biol* *28*, 1182-1194.

1123

1124 Chang, H., Lim, J., Ha, M., and Kim, V.N. (2014). TAIL-seq: genome-wide
 1125 determination of poly(A) tail length and 3' end modifications. *Mol Cell* *53*, 1044-
 1052.

1126

1127 Chen, J., Melton, C., Suh, N., Oh, J.S., Horner, K., Xie, F., Sette, C., Blelloch, R., and
 1128 Conti, M. (2011). Genome-wide analysis of translation reveals a critical role for
 1129 deleted in azoospermia-like (Dazl) at the oocyte-to-zygote transition. *Genes Dev*
25, 755-766.

1130

1131 Chen, L., Dumelie, J.G., Li, X., Cheng, M.H., Yang, Z., Laver, J.D., Siddiqui, N.U.,
 1132 Westwood, J.T., Morris, Q., Lipshitz, H.D., *et al.* (2014). Global regulation of
 1133 mRNA translation and stability in the early *Drosophila* embryo by the Smaug
 RNA-binding protein. *Genome Biol* *15*, R4.

1134

1135 Chu, T., Henrion, G., Haegeli, V., and Strickland, S. (2001). Cortex, a *Drosophila* gene
 1136 required to complete oocyte meiosis, is a member of the Cdc20/fizzy protein
 family. *Genesis* *29*, 141-152.

1137

1138 Courtot, C., Fankhauser, C., Simanis, V., and Lehner, C.F. (1992). The *Drosophila* cdc25
 homolog twine is required for meiosis. *Development* *116*, 405-416.

1139

1140 Cui, J., Sackton, K.L., Horner, V.L., Kumar, K.E., and Wolfner, M.F. (2008). Wispy, the
 1141 *Drosophila* homolog of GLD-2, is required during oogenesis and egg activation.
Genetics *178*, 2017-2029.

- 1142 Cui, J., Sartain, C.V., Pleiss, J.A., and Wolfner, M.F. (2013). Cytoplasmic
1143 polyadenylation is a major mRNA regulator during oogenesis and egg activation
1144 in *Drosophila*. *Dev Biol* 383, 121-131.
- 1145 Dobin, A., Davis, C.A., Schlesinger, F., Drenkow, J., Zaleski, C., Jha, S., Batut, P.,
1146 Chaisson, M., and Gingeras, T.R. (2013). STAR: ultrafast universal RNA-seq
1147 aligner. *Bioinformatics* 29, 15-21.
- 1148 Dunn, J.G., Foo, C.K., Belletier, N.G., Gavis, E.R., and Weissman, J.S. (2013).
1149 Ribosome profiling reveals pervasive and regulated stop codon readthrough in
1150 *Drosophila melanogaster*. *Elife* 2, e01179.
- 1151 Ernst, J., and Bar-Joseph, Z. (2006). STEM: a tool for the analysis of short time series
1152 gene expression data. *BMC Bioinformatics* 7, 191.
- 1153 Fenger, D.D., Carminati, J.L., Burney-Sigman, D.L., Kashevsky, H., Dines, J.L., Elfring,
1154 L.K., and Orr-Weaver, T.L. (2000). PAN GU: a protein kinase that inhibits S
1155 phase and promotes mitosis in early *Drosophila* development. *Development* 127,
1156 4763-4774.
- 1157 Greenspan, R.J. (1997). Fly pushing : the theory and practice of *Drosophila* genetics
1158 (Plainview, N.Y., Cold Spring Harbor Laboratory Press).
- 1159 Harrison, M.M., and Eisen, M.B. (2015). Transcriptional Activation of the Zygotic
1160 Genome in *Drosophila*. *Curr Top Dev Biol* 113, 85-112.
- 1161 Horner, V.L., and Wolfner, M.F. (2008). Transitioning from egg to embryo: triggers and
1162 mechanisms of egg activation. *Dev Dyn* 237, 527-544.
- 1163 Hughes, S.E., Gilliland, W.D., Cotitta, J.L., Takeo, S., Collins, K.A., and Hawley, R.S.
1164 (2009). Heterochromatic threads connect oscillating chromosomes during
1165 prometaphase I in *Drosophila* oocytes. *PLoS Genet* 5, e1000348.
- 1166 Igreja, C., and Izaurralde, E. (2011). CUP promotes deadenylation and inhibits decapping
1167 of mRNA targets. *Genes Dev* 25, 1955-1967.
- 1168 Ingolia, N.T., Ghaemmaghami, S., Newman, J.R., and Weissman, J.S. (2009). Genome-
1169 wide analysis in vivo of translation with nucleotide resolution using ribosome
1170 profiling. *Science* 324, 218-223.
- 1171 Ivshina, M., Lasko, P., and Richter, J.D. (2014). Cytoplasmic polyadenylation element
1172 binding proteins in development, health, and disease. *Annu Rev Cell Dev Biol* 30,
1173 393-415.
- 1174 Jacobs, H.W., Knoblich, J.A., and Lehner, C.F. (1998). *Drosophila* Cyclin B3 is required
1175 for female fertility and is dispensable for mitosis like Cyclin B. *Genes Dev* 12,
1176 3741-3751.

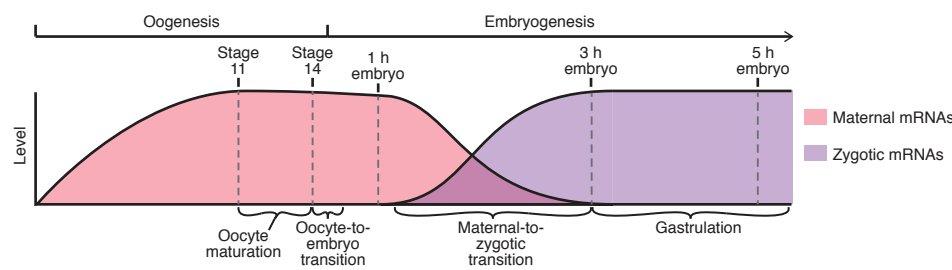
- 1177 Jan, C.H., Friedman, R.C., Ruby, J.G., and Bartel, D.P. (2011). Formation, regulation and
1178 evolution of *Caenorhabditis elegans* 3'UTRs. *Nature* *469*, 97-101.
- 1179 Kadyrova, L.Y., Habara, Y., Lee, T.H., and Wharton, R.P. (2007). Translational control
1180 of maternal Cyclin B mRNA by Nanos in the *Drosophila* germline. *Development*
1181 *134*, 1519-1527.
- 1182 Kronja, I., Whitfield, Z.J., Yuan, B., Dzeyk, K., Kirkpatrick, J., Krijgsveld, J., and Orr-
1183 Weaver, T.L. (2014a). Quantitative proteomics reveals the dynamics of protein
1184 changes during *Drosophila* oocyte maturation and the oocyte-to-embryo transition.
1185 *Proc Natl Acad Sci U S A* *111*, 16023-16028.
- 1186 Kronja, I., Yuan, B., Eichhorn, S.W., Dzeyk, K., Krijgsveld, J., Bartel, D.P., and Orr-
1187 Weaver, T.L. (2014b). Widespread changes in the posttranscriptional landscape at
1188 the *Drosophila* oocyte-to-embryo transition. *Cell Rep* *7*, 1495-1508.
- 1189 Liang, H.L., Nien, C.Y., Liu, H.Y., Metzstein, M.M., Kirov, N., and Rushlow, C. (2008).
1190 The zinc-finger protein Zelda is a key activator of the early zygotic genome in
1191 *Drosophila*. *Nature* *456*, 400-403.
- 1192 Lieberfarb, M.E., Chu, T., Wreden, C., Theurkauf, W., Gergen, J.P., and Strickland, S.
1193 (1996). Mutations that perturb poly(A)-dependent maternal mRNA activation
1194 block the initiation of development. *Development* *122*, 579-588.
- 1195 McGrew, L.L., Dworkin-Rastl, E., Dworkin, M.B., and Richter, J.D. (1989). Poly(A)
1196 elongation during *Xenopus* oocyte maturation is required for translational
1197 recruitment and is mediated by a short sequence element. *Genes Dev* *3*, 803-815.
- 1198 Nakamura, A., Sato, K., and Hanyu-Nakamura, K. (2004). *Drosophila* cup is an eIF4E
1199 binding protein that associates with Bruno and regulates *oskar* mRNA translation
1200 in oogenesis. *Dev Cell* *6*, 69-78.
- 1201 Nelson, M.R., Leidal, A.M., and Smibert, C.A. (2004). *Drosophila* Cup is an eIF4E-
1202 binding protein that functions in Smaug-mediated translational repression. *Embo J*
1203 *23*, 150-159.
- 1204 Newton, F.G., Harris, R.E., Sutcliffe, C., and Ashe, H.L. (2015). Coordinate post-
1205 transcriptional repression of Dpp-dependent transcription factors attenuates signal
1206 range during development. *Development* *142*, 3362-3373.
- 1207 Pesin, J.A., and Orr-Weaver, T.L. (2007). Developmental role and regulation of cortex, a
1208 meiosis-specific anaphase-promoting complex/cyclosome activator. *PLoS Genet*
1209 *3*, e202.
- 1210 Pique, M., Lopez, J.M., Foissac, S., Guigo, R., and Mendez, R. (2008). A combinatorial
1211 code for CPE-mediated translational control. *Cell* *132*, 434-448.

- 1212 Qin, X., Ahn, S., Speed, T.P., and Rubin, G.M. (2007). Global analyses of mRNA
1213 translational control during early *Drosophila* embryogenesis. *Genome Biol* 8, R63.
- 1214 Richter, J.D. (2007). CPEB: a life in translation. *Trends Biochem Sci* 32, 279-285.
- 1215 Salles, F.J., Lieberfarb, M.E., Wreden, C., Gergen, J.P., and Strickland, S. (1994).
1216 Coordinate initiation of *Drosophila* development by regulated polyadenylation of
1217 maternal messenger RNAs. *Science* 266, 1996-1999.
- 1218 Semotok, J.L., Cooperstock, R.L., Pinder, B.D., Vari, H.K., Lipshitz, H.D., and Smibert,
1219 C.A. (2005). Smaug recruits the CCR4/POP2/NOT deadenylase complex to
1220 trigger maternal transcript localization in the early *Drosophila* embryo. *Curr Biol*
1221 15, 284-294.
- 1222 Shamanski, F.L., and Orr-Weaver, T.L. (1991). The *Drosophila* plutonium and pan gu
1223 genes regulate entry into S phase at fertilization. *Cell* 66, 1289-1300.
- 1224 Sheets, M.D., Fox, C.A., Hunt, T., Vande Woude, G., and Wickens, M. (1994). The 3'-
1225 untranslated regions of c-mos and cyclin mRNAs stimulate translation by
1226 regulating cytoplasmic polyadenylation. *Genes Dev* 8, 926-938.
- 1227 Spradling, A.C. (1993). Developmental Genetics of Oogenesis. In *The Development of*
1228 *Drosophila Melanogaster*, M.A. Bate, A., ed. (Woodbury, Cold Spring Harbor
1229 Laboratory Press), pp. 1-70.
- 1230 Subtelny, A.O., Eichhorn, S.W., Chen, G.R., Sive, H., and Bartel, D.P. (2014). Poly(A)-
1231 tail profiling reveals an embryonic switch in translational control. *Nature* 508, 66-
1232 71.
- 1233 Swan, A., and Schupbach, T. (2007). The Cdc20 (Fzy)/Cdh1-related protein, Cort,
1234 cooperates with Fzy in cyclin destruction and anaphase progression in meiosis I
1235 and II in *Drosophila*. *Development* 134, 891-899.
- 1236 Tadros, W., Goldman, A.L., Babak, T., Menzies, F., Vardy, L., Orr-Weaver, T., Hughes,
1237 T.R., Westwood, J.T., Smibert, C.A., and Lipshitz, H.D. (2007). SMAUG is a
1238 major regulator of maternal mRNA destabilization in *Drosophila* and its
1239 translation is activated by the PAN GU kinase. *Dev Cell* 12, 143-155.
- 1240 Tadros, W., and Lipshitz, H.D. (2009). The maternal-to-zygotic transition: a play in two
1241 acts. *Development* 136, 3033-3042.
- 1242 Temme, C., Simonelig, M., and Wahle, E. (2014). Deadenylation of mRNA by the
1243 CCR4-NOT complex in *Drosophila*: molecular and developmental aspects. *Front*
1244 *Genet* 5, 143.
- 1245 Temme, C., Zhang, L., Kremmer, E., Ihling, C., Chartier, A., Sinz, A., Simonelig, M.,
1246 and Wahle, E. (2010). Subunits of the *Drosophila* CCR4-NOT complex and their
1247 roles in mRNA deadenylation. *RNA* 16, 1356-1370.

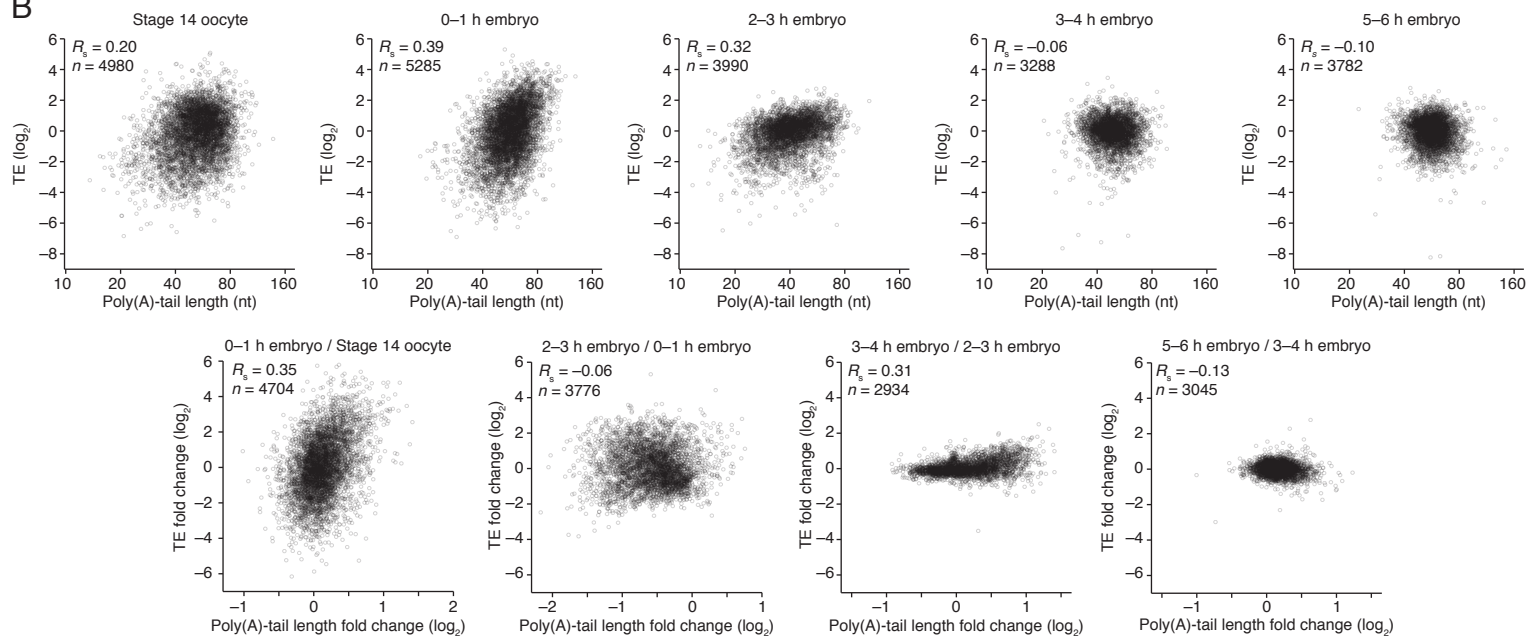
- 1248 Vardy, L., and Orr-Weaver, T.L. (2007a). The *Drosophila* PNG kinase complex regulates
1249 the translation of *cyclin B*. *Dev Cell* *12*, 157-166.
- 1250 Vardy, L., and Orr-Weaver, T.L. (2007b). Regulating translation of maternal messages:
1251 multiple repression mechanisms. *Trends Cell Biol* *17*, 547-554.
- 1252 Von Stetina, J.R., and Orr-Weaver, T.L. (2011). Developmental control of oocyte
1253 maturation and egg activation in metazoan models. *Cold Spring Harb Perspect*
1254 *Biol* *3*, a005553.
- 1255 Von Stetina, J.R., Tranguch, S., Dey, S.K., Lee, L.A., Cha, B., and Drummond-Barbosa,
1256 D. (2008). alpha-Endosulfine is a conserved protein required for oocyte meiotic
1257 maturation in *Drosophila*. *Development* *135*, 3697-3706.
- 1258 Weill, L., Belloc, E., Bava, F.A., and Mendez, R. (2012). Translational control by
1259 changes in poly(A) tail length: recycling mRNAs. *Nat Struct Mol Biol* *19*, 577-
1260 585.
- 1261
- 1262

Figure 1

A



B



C

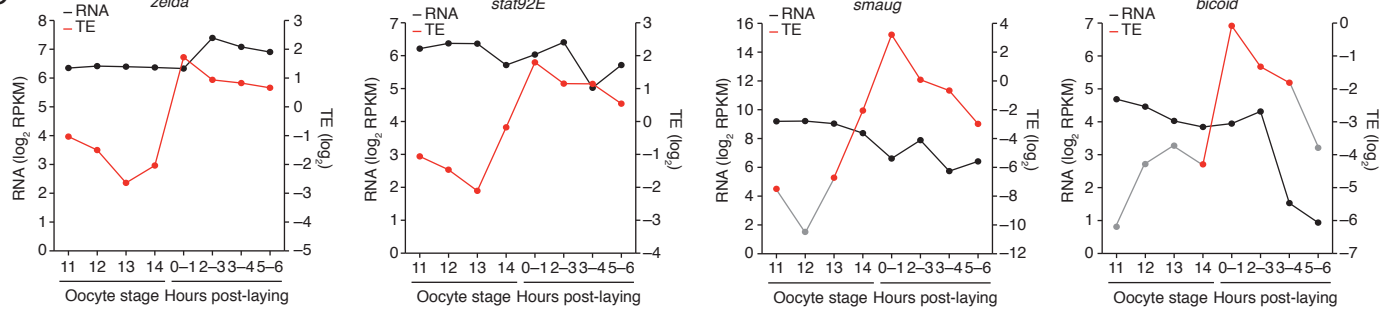


Figure 2

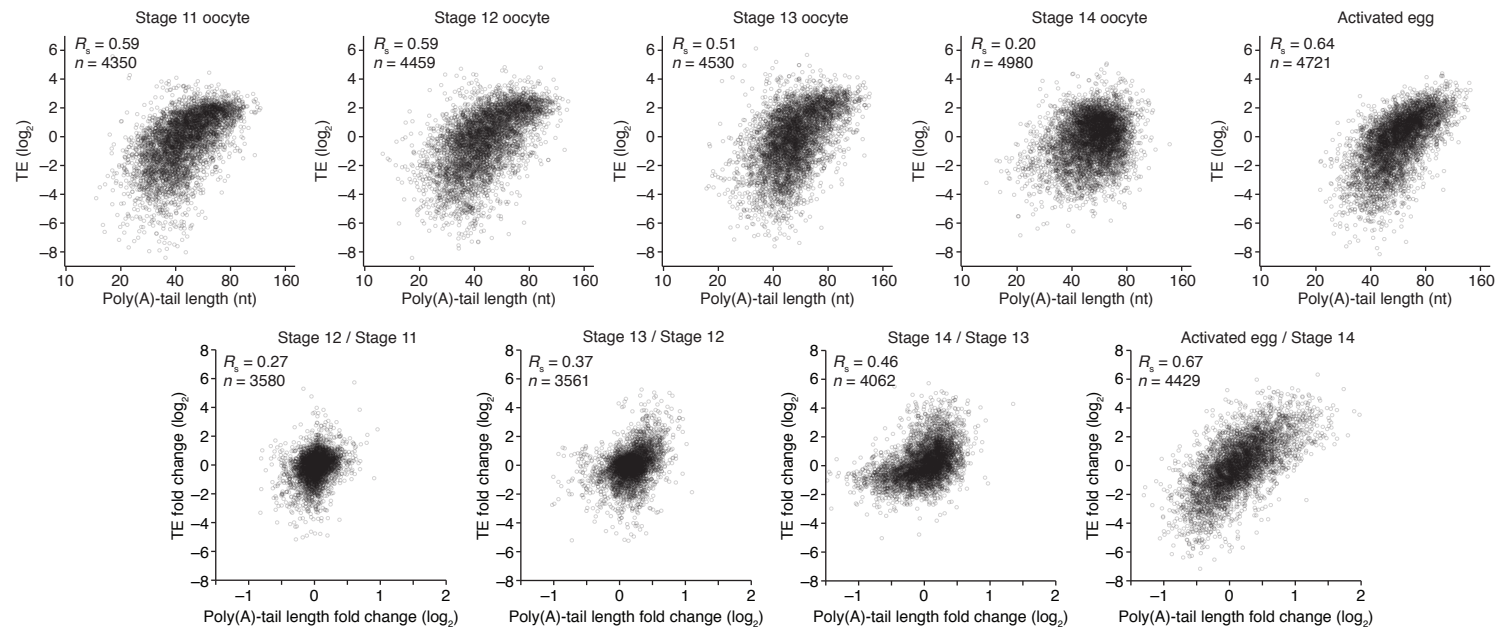
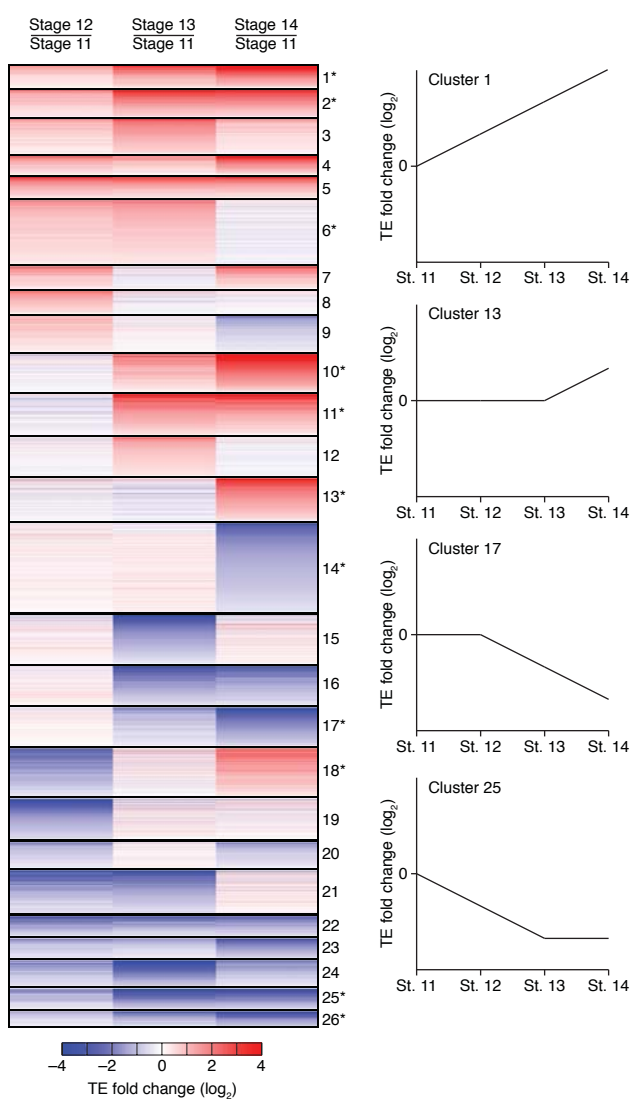


Figure 3

A



B

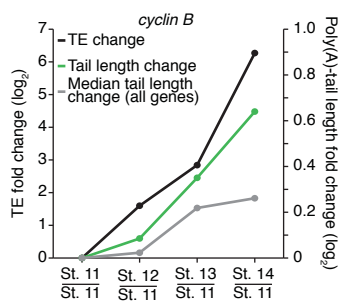


Figure 4

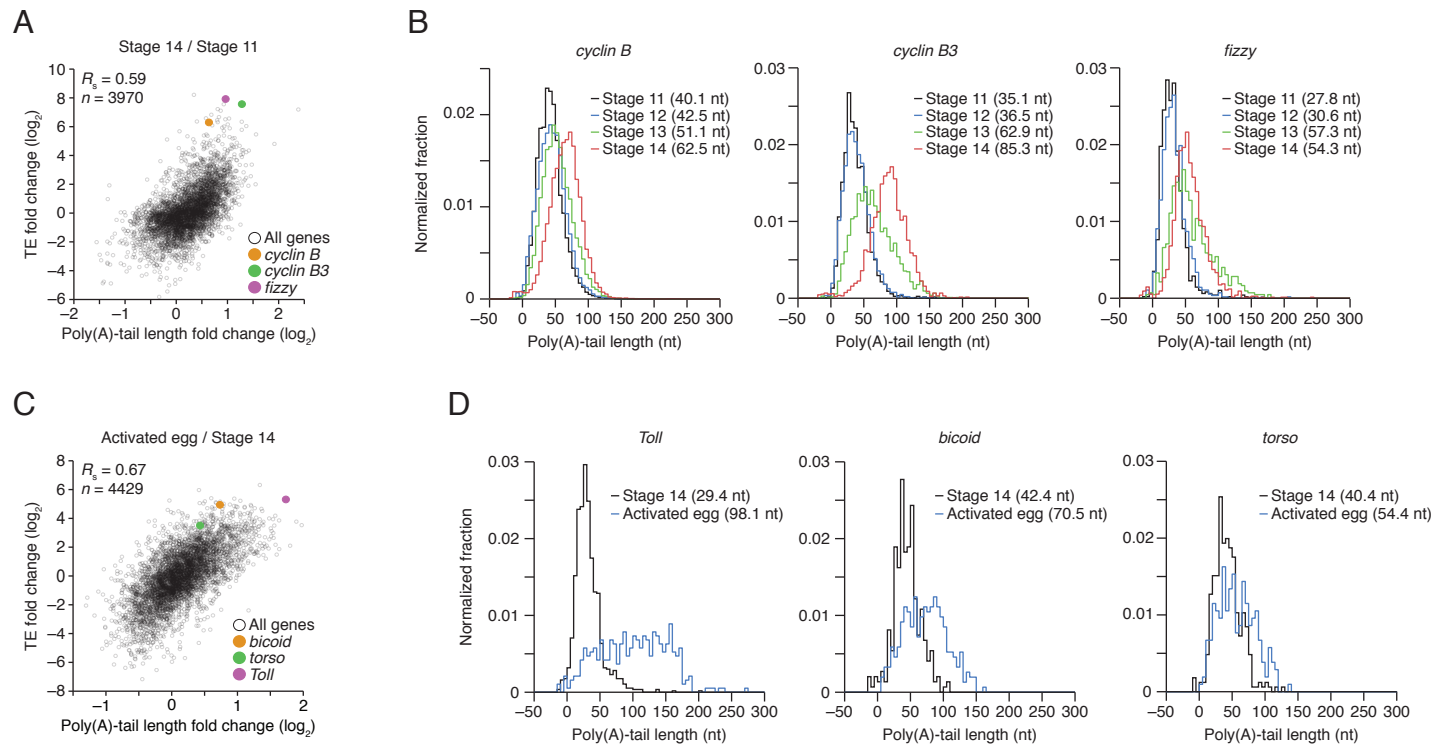


Figure 5

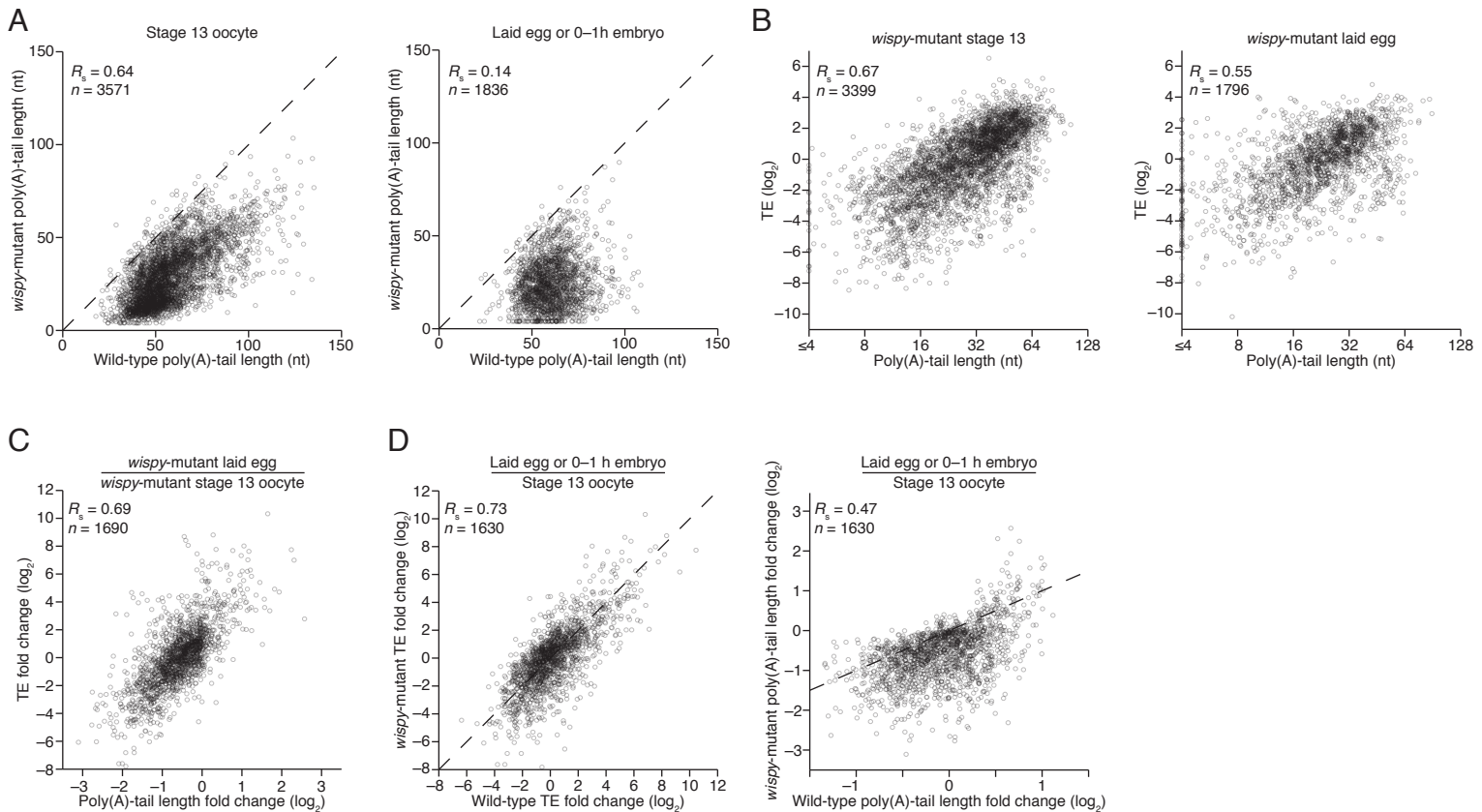
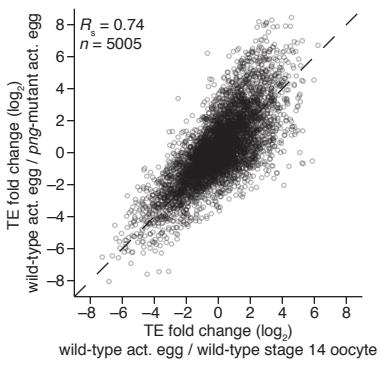
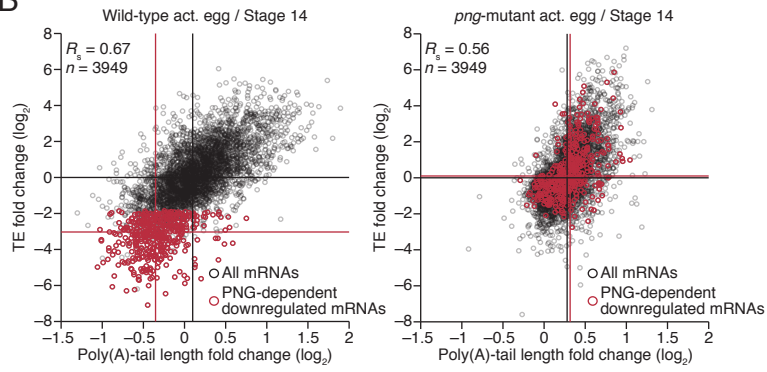


Figure 6

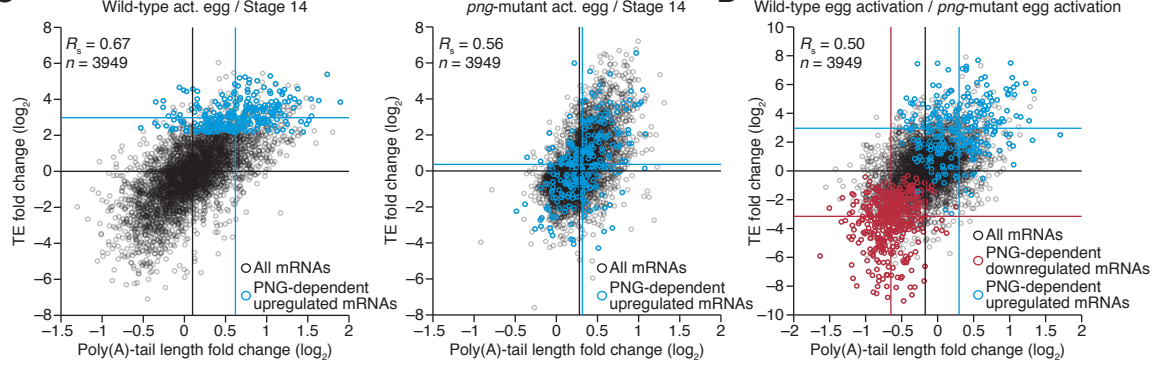
A



B



C



D

Figure 7

